

TANGLED WEBS

Evolutionary Dynamics on Fitness Landscapes with Neutrality

MSc Dissertation

Lionel Barnett (lionelb@cogs.susx.ac.uk)

MSc in Evolutionary and Adaptive Systems, Summer, 1997

Supervisor: Inman Harvey (inmanh@cogs.susx.ac.uk)

School of Cognitive Sciences

University of East Sussex

Brighton

Contents

Abstract

- 1. Introduction**
- 2. Landscape Structure**
 - 2.1. Measuring Neutrality**
 - 2.2. The Auto-correlation Function**
- 3. Abstract Landscapes Models with Neutrality**
 - 3.1. The NKp Family of Correlated Landscapes with Neutrality**
 - 3.2. The RNN Family of Landscapes - Walking the Hypercube**
- 4. Population Dynamics**
- 5. Simulation results**
 - 5.1. Population Dynamics on RNN Landscapes**
 - 5.2. Population Dynamics on NKp Landscapes**
- 6. Conclusions**

Acknowledgements

References

Figures

Appendix A

Appendix B

After a while your adversaries and competitors will give up trying to think of alternative hypotheses, or else will grow old and die, and then your hypothesis will become accepted. Sounds crazy, we know, but that's how science works!

- Numerical Recipes in C

Abstract

The bulk of research on the dynamics of populations of genotypes evolving on fitness landscapes has concentrated on the rôle of correlation and landscape ruggedness as a putative indicator of the qualitative dynamics. There is, however, a small but growing awareness amongst population geneticists (through Motoo Kimura's Neutral Theory of molecular evolution [16, 3]) and molecular biologists (Eigen, Schuster, *et. al.* [5, 2, 18]) of the importance of neutral mutation as a significant factor in evolutionary dynamics. This awareness has thus far not extended to the GA community. Of particular interest is the notion of *neutral networks* of selectively neutral genotypes which percolate a fitness landscape - recent work on RNA folding landscapes characterises their structure in terms of such networks [21, 6, 20, 12, 13, 1]. There is at present a lack of computationally tractable abstract models demonstrating neutrality. In this paper we introduce two parametrised families of abstract landscapes: the NKp landscapes, based on the NK family of abstract landscapes [15], allow tuning of the degree of neutrality whilst leaving invariant the auto-correlation function [24, 23, 15]. The RNN (Random Neutral Network) landscapes, constructed by mutually-avoiding random walks, feature percolating neutral networks of specifiable size and neutral dimension. The statistical structure of these landscapes is examined and related to the characteristic dynamics of populations evolving on them. Several conjectures regarding the auto-correlation function on NKp landscapes (relevant also to NK landscapes) are raised. Attention is drawn to the very different nature of population dynamics on landscapes with percolating neutral networks as compared to the dynamics on rugged multi-peaked landscapes. Qualitative similarities between population dynamics on RNN landscapes and RNA folding landscapes are highlighted. Finally, implications for biological research and for the application of GA's to optimisation problems are discussed.

1 Introduction

With the introduction of the notion of a fitness landscape by Sewall Wright evolutionary theory acquired a powerful and intuitively appealing metaphor. But a fitness landscape, it must be stressed, is above all an *abstraction*. Fitness landscapes *do not exist* in the world of real biology (or indeed real engineering or real chemistry). The basic idea of the abstraction is that the potential for reproduction of evolving entities can somehow be quantified - that we can attach a *number* to a genotype and that this number specifies, according to some (probably stochastic, iterative) algorithm, the number of copies of that genotype that we can expect to find in the next generation of genotypes. But does nature attach numbers to genotypes? Does nature run iterative stochastic algorithms? These questions may seem frivolous, but they beg serious consideration. How, for instance, are we to attach a "fitness" to the genotype of a real organism if we cannot possibly take into account the enormous complexity of the physical world which will ultimately decide how many offspring that organism really does have?

A common approach to this dilemma deploys what one might term "black box" models - we admit that we cannot know the inner workings of the real world in all its stupendous detail, but that on some gross level the critical phenomena involved are amenable to a *statistical* description. This is precisely the approach taken in statistical mechanics. We don't attempt to describe what every particle in a gas is doing at each moment; we speak, instead, of statistical properties of the ensemble of particles - of temperature, pressure and entropy. We use the language of probability, of random variables. Likewise in constructing an NK landscape [15], we are saying: "I don't know the precise fitness contribution of an allele, or the configuration of epistatic linkage, so I'll *approximate* these things by assigning them at random". The hope is that (perhaps with the Central Limit Theorem on our side) we will thus end up with a model that reflects at least some characteristics of the real world. The landscape models in this study are of this nature and should be understood in this spirit.

Another approach, applicable where the physics of the system under investigation is tractable to experimental analysis, is to construct fitness landscapes and evolutionary algorithms modelled as precisely as is feasible on the physical system. RNA folding landscapes [22] and flow-reactor models [13, 6] fall into this category.

Ultimately the only resolution of these issues lies in the acceptance of fitness landscapes as abstract models that are significant, not in their own right, but only insofar as they assist us in understanding and predicting the world as it really is. Like any mathematical model our models may be "interesting" or even "beautiful"; they may acquire a cachet, a life of their own in the scientific consciousness, but *are they useful?* The real space-time continuum is *not* a Riemannian manifold, real photons are *not* operators on a Hilbert space; but these abstractions have been enormously successful in helping us make sense of the *real* space-time continuum, of *real* photons. So may it be with fitness landscapes.

Fitness landscapes suggest a methodology for analysis of the dynamical process that characterises an evolving system: if a fitness landscape is indeed a reasonable abstraction then an evolving system may be modelled as a quantifiable stochastic process on some abstract landscape. As such, we may expect it to be constrained by the statistical properties of the landscape. The question then arises: what statistical features of a fitness landscape are relevant to the dynamics of a population evolving on that landscape, and in what manner do they constrain the dynamics?

In attempting to address these questions a picture has become somewhat ingrained in the collective mind of biologists and GA researchers alike, of a fitness landscape as a rugged terrain distinguished by peaks of relatively high fitness separated by valleys of relatively low fitness [15]. This picture leads to the view of evolutionary dynamics on such a landscape in terms of the following scenario: selection pressure will tend to pull a population up the highest hill it chances upon, while genetic operators (mutation, recombination, etc.) counteract this tendency by scattering new genotypes around the locality of the population.

But this poses a problem which affects both the biologist and the GA specialist: if selective pressure is strong enough (relative to the disruptive effects of genetic operators) to drag a population up a hill, it is also likely to be strong enough to hold it there! How, then, is an evolving population to avoid becoming "trapped" on a local hilltop? For the GA worker seeking to optimise a multi-peaked function this is a practical issue and the literature abounds with schemes to avoid the dilemma [9]. For the biologist it is a serious theoretical conundrum, as populations in nature do not seem (in the long run at least) to suffer this fate [3]. It might be claimed that this can be easily explained by co-evolution and environmental change but another possibility must be considered - our picture of a fitness landscape as a rugged hilly terrain is misleading and in need of an overhaul.

Comparatively recent developments in evolutionary theory and molecular biology have all pointed to the importance of *selective neutrality* as a significant factor in evolutionary dynamics. This work includes Motoo Kimura's Neutral Theory of molecular evolution [16, 3], Manfred Eigen's analysis of molecular "quasispecies" [5, 2, 18] and recent developments in the understanding of RNA evolution both *in vitro*, in simulation and analytically [21, 22, 6, 20, 12, 13, 1]. A picture emerges of populations engaged not in hill-climbing but rather drifting along connected networks of neutral genotypes, with sporadic jumps between networks. These *neutral networks* are of particular significance if they "percolate" the landscape - i.e. they come arbitrarily close to almost every other neutral network - for this raises the possibility that (given enough time) genotypes of almost *any* possible fitness value can ultimately be attained by the population. The scenario of a population trapped on a local hilltop vanishes.

It is this new paradigm of evolutionary dynamics which we examine in this paper. It has yet to make a significant impact on the scientific community; it is hoped that the model landscapes, studies of population dynamics and analytic techniques presented here may assist in gaining insight into the nature of neutral evolution.

At this point we mention several facets of evolution on fitness landscapes which we specifically exclude from the ambit of this study - not because they are of no importance to a real understanding of evolution, but rather that they would introduce complexities beyond what could be dealt with here and distract from the specific issues we attempt to address. For this we offer no apology, merely the hope that these *caveats* may be addressed in future studies.

The first issue is that of static vs. dynamic landscapes. In nature, apart from change of environment over geological time-spans, evolution is almost always *co*-evolution and any attempt to model

evolution on a static landscape is bound to be unrealistic. It might be argued that static landscapes may be acceptable models if the time-scale of environmental change is much greater than that of evolutionary change and co-evolution is not significant. It is not clear whether this is ever the case in nature. All model landscapes in this paper are static.

Secondly fitness, as a mediator of selection for reproduction can surely never be precise in nature - real fitness is noisy - this must be considered distinct from any stochasticity present in the selection mechanism of an evolutionary algorithm. It is often not appreciated that noise may dramatically alter the dynamics of a complex dynamical system. Our landscapes prescribe, and our evolutionary algorithm presumes, a precise and pre-ordained fitness value for every genotype.

Thirdly our genotypes are all binary and fixed-length. The binary restriction is arguably not too inadequate when it comes to modelling systems such as RNA folding; it would probably be woefully deficient in a model of RNA or DNA protein coding, where the number of allelic possibilities is vast. The fixed-length restriction could possibly be justified on the grounds that length-change mutation seems to be comparatively rare in nature. Our genotypes are, furthermore, rather short (in the region of 20 loci); this restriction was imposed by time and computational constraints. It is not clear how some of the phenomena observed might scale to more realistic sequence lengths.

Next we limit our "genetic operators" to mutation alone. Our genotypes are all haploid and reproduction is asexual. This merits some comment. In the GA literature dating back to John Holland [11, 9] there has been a perception of recombination (crossover) as the driving force behind evolutionary search, with mutation taking a back seat as an insurance policy against permanent allelic loss. It is not clear why mutation has been thus relegated, nor that recombination is necessarily effective in search. From the biological point of view there are many organisms for which recombination rarely or never occurs during reproduction. Molecular biology, furthermore, offers many scenarios of non-recombinative reproduction.

Finally we restrict ourselves to a single "fitness-proportional" evolutionary algorithm. Again, the actual mechanics of selection in natural systems tends to be inscrutable [3], so this choice is motivated more through being a standard and comparatively well-understood model than by biological considerations. It may be noted, though, that in the field of GA's in optimisation [9] one is as likely to encounter rank-based selective schemes, which appear to offer some advantages over fitness-proportional schemes in optimisation applications. The results in this paper cannot be expected to extend *mutatis mutandis* to other evolutionary algorithms.

Section 2 introduces the tools that will be used to analyse the structure of our landscapes, particularly as regards neutrality. Section 3 introduces two rather different parametrised families of landscapes with "tuneable" neutrality and investigates their structure. Section 4 presents some methods for analysing population dynamics on landscapes with neutrality and Section 5 applies these methods to the landscape models introduced in Section 3. Section 6 discusses the results and their implications as regards possible application. Areas for further study are also suggested. Appendix A contains some mathematical calculations, while Appendix B contains a source listing of the LSCAPE program used to compute all results contained in this paper.

2 Landscape Structure

Much of the literature on fitness landscape structure deals with the concept of *ruggedness* of a landscape [15, 24]. Intuitively this addresses the question: given two "neighbouring" genotypes on a landscape, how similar are their fitness values likely to be? The main reason for this emphasis seems to be the perception of a fitness landscape as a vast hilly terrain, on which an evolving population

samples a comparatively tiny fraction of genotypes at any one time for fitter variants. Evolutionary search, if it is not to be random, is likely to be localised in a small neighbourhood within the landscape. It is then natural to inquire what the chances are of finding a better (i.e. higher fitness) genotype than currently exists in the population, by searching the neighbourhood of the current population. If fitness values can vary wildly even within small neighbourhoods, it is perceived that the search, even locally, is hardly better than random. If, on the other hand, fitness varies only gradually within small neighbourhoods, the possibility exists for local hill-climbing.

It has already been mentioned in the Introduction that there are reasons to believe that this picture may be misleading when there is large-scale neutrality, which is frequently the case for both biological and artificial fitness landscapes. Nor does it address the issue of how a *particular* evolutionary algorithm actually searches, nor indeed whether local hill-climbing is actually desirable at all... Nevertheless it is a *de facto* standard technique to analyse landscapes in terms of ruggedness and in Section 2.2 below we introduce the most commonly encountered measure of landscape ruggedness, the **auto-correlation function**. In Section 3.1 we shall see that on some families of fitness landscapes this measure possesses some counter-intuitive properties and that consequently it may, on its own, be of limited relevance to evolutionary dynamics. Here a variant of the conventional auto-correlation function taking into account landscape neutrality is suggested. Before that, in Section 2.1 we introduce some analytical measures of landscape neutrality.

All fitness landscapes in this paper are based on fixed-length binary bit-string genotypes. Most of the analysis and actual landscapes, however, generalise quite straightforwardly to the case of multiple alleles. A **fitness landscape** G of sequence length N is then formally defined to be a mapping $f: Q^N \rightarrow \mathbf{R}$ where Q^N denotes the binary N -hypercube and \mathbf{R} is the set of real numbers. By abuse of notation we generally identify G with the underlying space Q^N (so $|G| = 2^N$) and refer to the mapping f as the **fitness function**. The **fitness** of a genotype $g \in G$ is then given by $f(g)$. We will often simply refer to a fitness landscape G , the fitness function $f(\dots)$ being implicitly assumed.

There is a natural metric, **Hamming distance**, on Q^N defined to be the number of **loci** (bit positions)

at which two genotypes differ. Precisely, $h(g, g') \equiv \sum_{i=1}^N \delta(g_i, g'_i)$ where g_i denotes the allele (0 or 1)

at the i -th locus of g and $\delta(a, b) \equiv \begin{cases} 1 & \text{if } a = b \\ 0 & \text{if } a \neq b \end{cases}$ Hamming distance thus introduces a structure of

locality on a fitness landscape¹. Hamming distance is often referred to in terms of **mutation**. If $h(g, g') = d$ we say that g' is a (d -bit) mutation of g (and vice-versa, since the relationship is symmetric). We also sometimes say that g and g' are (d -bit) **neighbours**.

A point of confusion worth addressing at this stage is that measures of landscape structure are often treated as statistical quantities associated with random variables when they are, in fact, precisely defined quantities associated with a particular landscape. An example might be the mean fitness \bar{f} of a fitness landscape. This is simply a real number associated with a landscape, defined by

$\bar{f} \equiv \frac{1}{|G|} \sum_{g \in G} f(g)$. It is, however, often treated as the mean, or expected value (in the sense of

probability theory) of a putative random variable, presumably the fitness function f itself! But f is evidently not a random variable, so \bar{f} cannot be a mean in the sense of probability theory. There are two distinct (and often confused) senses in which f might be treated as a random variable. The first is that the sum over G in the definition of \bar{f} may be practically impossible to compute, due to the size (2^N) of G . Hence in practice \bar{f} is estimated by summing over a sample of genotypes in G . This

suggests defining a (discrete) random variable F , say, by setting $\mathbf{P}(F = x) \equiv \frac{|G^x|}{|G|}$ where

$G^x \equiv \{g \in G \mid f(g) = x\}$. In this sense \bar{f} as defined above is indeed the mean of the random variable F .

¹ It is sometimes claimed that if other genetic operators than mutation are being discussed Hamming distance may not be the most natural or suitable metric structure for a landscape. This point is, however, open to debate...

However, \bar{f} is often intended to be something quite different; namely, it is often the case that a *parametrised family* $\Gamma = \{G^{\lambda, \lambda', \lambda'', \dots}\}$ of fitness landscapes is being discussed, where the parameters $\lambda, \lambda', \lambda'', \dots$ are themselves (jointly distributed) random variables (which may be discrete or continuous). For example the ensemble of all NK landscapes for fixed N and K falls into this category, where the λ 's correspond to the configuration of epistatic links and the fitness table values (see Section 3.1 below). Then we can consider \bar{f} to be a random variable over the sample space Γ and its mean, variance, etc. are well-defined. We attempt to maintain this distinction by using angle-brackets for this latter case - we would thus write not \bar{f} but $\langle \bar{f} \rangle$ or even $\langle \bar{f} \rangle_{\Gamma}$ if we wish to make the dependence on the parametrised family Γ clear.

2.1 Measuring Neutrality

Given a fitness landscape G we describe a (1-bit) mutation (g,g') as **neutral** iff $f(g) = f(g')$. This induces a natural partitioning of G, whereby g and g' are in the same equivalence class iff there is a sequence of neutral mutations connecting g and g'; i.e. there are genotypes $g \equiv g^{(0)}, g^{(1)}, g^{(2)}, \dots, g^{(n)} \equiv g'$ such that $g^{(\alpha)}$ is a 1-mutant neighbour of $g^{(\alpha-1)}$ for $\alpha = 1, 2, \dots, n$ and $f(g) \equiv f(g^{(0)}) = f(g^{(1)}) = f(g^{(2)}) = \dots = f(g^{(n)}) \equiv f(g')$. The **neutral networks** of the fitness landscape are defined to be the equivalence classes of this partitioning. Note that we could define a "coarser" partitioning of G by specifying g and g' to be in the same class iff their fitness values are equal. Under the metric induced by Hamming distance the neutral networks are just the connected components (in the topological sense) of the equivalence classes of this coarser partitioning².

A word of caution - the "network" terminology may well be misleading. If the frequency of neutral mutation is low, there are likely to be very many neutral networks comprising a few, or even single genotypes. Even if there is high neutrality the neutral networks may not resemble networks as much as large clusters.

Given a genotype $g \in G$ we define the **neutral dimension** of g to be the number of neutral mutations of g minus 1. The reason for subtracting 1 is to facilitate the image of a neutral network of given dimension, where we define the neutral dimension of a neutral network to be the mean of the neutral dimensions of its constituent genotypes (see Figure 2.1.1).

Since the neutral dimensions of the genotypes along a neutral network may vary, we will also be interested in the variance of neutral dimension over a neutral network. In Section 4 we will see that neutral dimension turns out to be of particular significance to population dynamics on a landscape with high neutrality.

We would like to quantify the degree to which a neutral network "percolates" the fitness landscape. From the point of view of population dynamics, the question of interest is how many new "phenotypes" or fitness values can be reached within one (or a few) mutations of the network. Thus we define the **percolation index** (at distance d) of a neutral network to be the fraction of possible fitness values attainable within at most d mutations of some genotype on the network.

Precisely, we define the percolation index $\pi_H(d)$ of a neutral network $H \subset G$ to be $\frac{|H(d)|}{|F|}$ where

$H(d) \equiv \{f(g) \mid g \in G \text{ and } \exists g' \in H \text{ with } h(g, g') \leq d\}$ and $F \equiv \{f(g) \mid g \in G\}$. $\pi_H(d)$ is, unfortunately, expensive to compute in practice as it involves tabulation of all possible fitness values and the traversal of the entire neutral network. Huynen [12] has defined a stochastic procedure which measures the "innovation rate" along a random walk on a neutral network. The idea is to enumerate new fitness values or "innovations" encountered (i.e. which are $\leq d$ mutations away from the current

² In the RNA folding literature it is sometimes effectively this coarser partitioning that is used to define neutral networks, which thus need not be connected. In all fitness landscapes encountered in this paper the two partitionings generally "almost" coincide, and we sometimes conveniently confuse them...

genotype) on such a "neutral walk". The number of innovations may then be compared with the number of innovations on a *random* walk of the same length. The ratio of these numbers, when averaged over a large number of walks should then be roughly comparable with $\pi_H(d)$ as defined above³.

In Section 3 we will analyse the neutral network structure of our model landscapes in terms of the distributions of size, percolation index $\pi(1)$, mean neutral dimension and neutral dimension variance among the neutral networks on the various families of landscapes⁴. We also calculate theoretically where possible the probability that an arbitrary mutation is neutral.

2.2 The Auto-correlation Function

The auto-correlation function makes precise the notion of how similar nearby genotypes are in a fitness landscape. It is often defined in terms of fitness values at successive steps along random walks on the landscape [24, 15] but, as remarked in [23] "...it seems to be rather contrived to invoke a stochastic process in order to characterise a given function [i.e. the fitness function] defined on a finite set". We thus use the definition below, apparently first proposed in [5].

We first define the mean fitness of the landscape

$$\text{Eq 2.2.1} \quad \bar{f} \equiv \frac{1}{|G|} \sum_{g \in G} f(g)$$

the fitness variance

$$\text{Eq 2.2.2} \quad \sigma_f^2 = \frac{1}{|G|} \sum_{g \in G} (f(g) - \bar{f})^2$$

and for $d = 1, 2, \dots, N$ the set

$$\text{Eq 2.2.3} \quad G^2(d) \equiv \{(g, g') \in G \times G \mid h(g, g') = d\}$$

Thus $G^2(d)$ is the set of pairs of genotypes in G Hamming distance d apart. Note that $|G^2(d)| = \binom{N}{d} \cdot |G|$ since there are $\binom{N}{d}$ ways of flipping d loci of a bit-string of length N .

We now define for $d = 1, 2, \dots, N$ the auto-correlation function to be:

$$\text{Eq 2.2.4} \quad \rho(d) \equiv \frac{1}{\sigma_f^2 |G^2(d)|} \sum_{(g, g') \in G^2(d)} (f(g) - \bar{f})(f(g') - \bar{f})$$

For consistency we also define $\rho(0) \equiv 1$. For computational purposes we can estimate \bar{f} , σ_f^2 and $\rho(d)$ by sampling subsets of G and $G^2(d)$. The basic properties of $\rho(d)$ are that on a flat fitness landscape ($f = \text{constant}$) $\rho(d) = 1$ for all d (in the limit at least, since the formula yields $0/0$!) while on a completely uncorrelated landscape $\rho(d)$ will be close to 0. This can be made precise in the following manner: introducing the family Γ of landscapes where each $G \in \Gamma$ is specified by assigning fitness

³ This should at least be the case if the neutral network is "network-like". If it is more like a "clump" than a network, then neutral walks are likely to encounter comparatively fewer "innovations" and may not be a good indicator of percolation index as defined here.

⁴ For these landscapes the genotypes of zero fitness constitute a special case. Thus we generally omit the zero-fitness genotypes from our analysis of neutral networks.

values independently and uniformly randomly from $[0,1]$ to each genotype, we have $\langle \rho(d) \rangle_T = 0$ (c.f. the closing paragraph in the introduction to this Section).

The auto-correlation function has been quite thoroughly studied for some classes of landscapes [23, 24]. In particular, for a large family of "elementary" landscapes [23], the auto-correlation is exponential of the form $\rho(d) = a^{-d}$ for some constant a , and there is thus a natural "correlation length" for the landscape⁵.

As we shall see in Section 3.1, in the presence of large-scale neutrality the auto-correlation function appears to be inadequate on its own as a measure of landscape structure. The effect of neutrality on the correlation structure is indeed by no means clear-cut. If a landscape features extensive percolating networks, and particularly if they are of high neutral dimension, then on the one hand it might be expected that the correlations introduced by neutral mutations would tend to boost the correlation of neighbouring genotypes - effectively "smoothing" the landscape. On the other hand, percolation suggests that there is a high likelihood that genotypes of possibly uncorrelated fitness on different neutral networks can end up close together, with the effect of increasing ruggedness. In the next section we will see evidence that both these effects can occur, and indeed may even appear to "cancel each other out".

Nonetheless, there is evidence from RNA folding landscapes that percolating neutral networks and a significant correlation structure may well cohabit on a landscape [13, 12]. What seems to be required is a refinement of the auto-correlation function which takes neutrality into account.

One possibility that suggests itself is that in the definition of $\rho(d)$, rather than averaging over the set $G^2(d)$ defined in Eq. 2.2 3, we use instead the "no neutrals" alternative:

Eq 2.2.3a
$$G^2_{nn}(d) \equiv \{(g, g') \in G \times G \mid h(g, g') = d \text{ and } f(g) \neq f(g')\}$$

Thus we measure correlation of fitness of neighbouring genotypes picked from *different* neutral networks. Preliminary investigation suggests that an auto-correlation function defined in terms of this set may prove useful in characterising landscape structure, if considered in conjunction with the percolation index and neutral dimension⁶.

3 Abstract Landscapes Models with Neutrality

In this Section we introduce the landscape models on which our studies of evolutionary dynamics will be based.

3.1 The NKp Family of Correlated Landscapes with Neutrality

We begin by reviewing the construction of an NK landscape [15]. Let $N > 0$ be the length of the (binary) genotype and let $0 \leq K < N$. N and K are fixed during the construction. To each locus on the genotype (corresponding to a position $1 \leq i \leq N$ on the bit-string) we assign independently and at random K distinct loci (excluding the locus under consideration) - these loci are said to be *epistatically linked* to the locus i . The idea is that a locus i makes a contribution to the total fitness of the genotype which depends on the value of the allele (0 or 1) at i and the values of the alleles at each of the K loci epistatically linked to locus i . To each such combination of alleles (there are 2^{K+1} in all) a fitness contribution is assigned as a real number drawn independently and uniformly at random from

⁵ Contrary to popular belief the correlation function on NK landscapes is not exponential in form, although it does resemble an exponential for large K values. See Section 3.1 for more on this topic.

⁶ Preliminary tests also demonstrated that this "no neutrals" variant can, unlike the conventional function, distinguish between NKp landscapes (see Section 3.1) with different values of p .

the range [0,1]. We can think of this as the association of a *fitness table* F_i with each locus i . Given the sequence of alleles $\sigma = a_1 a_2 \dots a_{K+1}$ at the loci epistatically linked to locus i , the fitness contribution of locus i is then given by $F_i(\sigma)$. Figure 3.1.1 illustrates the situation. Here $N = 16$, $K = 3$ and the locus under consideration is at $i = 5$. The red arrows indicate epistatic links and a segment of the fitness table for locus 5 is pictured. For the genotype illustrated the sequence of alleles for locus 5 is $\sigma = 0110$ and the corresponding entry in the fitness table is $F_5(\sigma) = 0.305687$.

Finally, to calculate the fitness of an entire genotype the fitness contributions of all loci are summed and the result divided by N (the genotype length) to scale the fitness to the range [0,1]. In the above notation, if g is a genotype and $\sigma_i(g)$ the sequence of alleles at the loci epistatically linked to locus i on g , its is given by:

$$\text{Eq 3.1.1} \quad f(g) = \frac{1}{N} \sum_{i=1}^N F_i(\sigma_i(g))$$

In summary, an NK landscape is fully specified by N , K , the particular assignment of epistatic links and the contents of the N fitness tables.

The statistical properties of NK landscapes have been widely studied [15], and in particular the auto-correlation measure for NK landscapes is fairly well understood. The general picture is that for $K = 0$ an NK landscape is highly correlated. As K is increased the correlation drops off until for $K = N-1$ the landscape is completely uncorrelated.

It is clear from the construction procedure that there is (almost surely) *no neutral mutation* on an NK landscape - for if two genotypes differ at some locus the respective fitness contributions for that locus will be drawn from different fitness table entries which will (almost surely) be different. There is, however, a "natural" way to introduce neutrality into the model, via by the following biologically-inspired argument: the NK model assumes that *every possible* combination of alleles at the loci epistatically linked to a given locus gives rise to a positive contribution to genotype fitness. In nature, however, it seems likely that many (if not most) combinations of alleles will make *no* contribution to fitness (or be "lethal"). We could reflect this in the NK model by specifying that the fitness table entry corresponding to such an allelic combination be equal to zero. Thus motivated we proceed as follows: a new parameter $0 \leq p \leq 1$ is introduced to represent the probability that an arbitrarily allelic combination makes no contribution to fitness. Explicitly, when assigning values to the fitness tables we set each entry to 0 independently with probability p . If an entry is not set to zero it is assigned uniformly randomly from the range [0,1] as before. We refer to the resulting landscape as an **NK p landscape**. The case $p = 0$ corresponds to a normal NK landscape, while $p = 1$ corresponds to a completely flat landscape (all fitness table entries are zero).

It is evident that the possibility of neutral mutation arises in NK p landscapes. A calculation (see Appendix A.1) yields for the probability that an arbitrary mutation be neutral:

$$\text{Eq 3.1.2} \quad p_{\text{neutral}} = p^2 \left(1 - \frac{K}{N-1} (1-p^2) \right)^{N-1}$$

For large N (long genotypes) this is well approximated by:

$$\text{Eq 3.1.2'} \quad p_{\text{neutral}} \approx p^2 e^{-K(1-p^2)}$$

Thus the probability of a mutation being neutral is roughly independent of the genotype length for long genotypes. Figure 3.1.2 plots p_{neutral} (as calculated from Eq 3.1.2) against K and p for $N = 30$.

We now examine the expected number of neutral mutations per genotype. Since at each genotype there are N possible 1-bit mutations, the expected number of neutral mutations at each point in the landscape is Np_{neutral} . The problem is that while this gives us the *average* number of neutral mutations

per genotype it does not tell us how this quantity is distributed over the landscape, particularly with regard to fitness.

For a genotype g let us set $n(g)$ = number of neutral mutations at g , and $\zeta(g)$ = number of loci on g which make zero contribution to the fitness of g ; i.e. which yield a zero in the i -th fitness table. We have immediately that $f(g) \leq 1 - \frac{\zeta(g)}{N}$. But for a mutation at i to be neutral g must necessarily have a zero in its i -th fitness table. Thus:

$$\text{Eq 3.1.3} \quad n(g) \leq \zeta(g) \leq N(1-f(g)).$$

This implies that genotypes with higher fitness values will have a smaller number of neutral mutations.

Figure 3.1.3 plots the distributions of neutral mutations for genotypes falling into fitness bands for NKp landscapes with $N = 30$, $K = 4$ and $p = 0.9$. Note that this graph does not represent the *joint* distribution of fitness and neutral mutations. Each "slice" (corresponding to genotypes within a given fitness range) plots the distribution of neutral mutations *for genotypes within that fitness range*. The figures were derived from a sample of 1000 genotypes each from 1000 NKp landscapes.

We see that while the individual distributions are bell-shaped in appearance, the distribution means fall off roughly linearly with increasing fitness as suggested by Eq 3.1.3. The implication is that the "higher up" the landscape we go, the smaller the number of neutral mutations we are likely to encounter. Furthermore, for genotypes of high fitness a mutant is very likely to be a genotype with more zeros in the fitness tables than its neighbour (particularly with high epistasis), and hence of dramatically smaller fitness. Looked at another way, NKp landscapes become in a sense *more rugged* with increasing p .

Figures 3.1.4a-d give the (non-zero fitness) neutral net statistics for $N = 18$, $K = 4$ and $p = 0.99$, presented as joint distributions over fitness. [For small values of p the neutral networks are small and there is no percolation]. Results are compiled from averages over 100 landscapes. We see from Figure 3.1.4a that the neutral networks fall into two groups; there are numerous small networks and comparatively few large ones. The numbers of both fall off with increasing fitness. There is moderate percolation, again falling off with increasing fitness. Neutral dimension also appears to divide into two groups; these are likely to correspond to the large and small groups of networks. Neutral dimension decreases with increasing fitness. Variance of neutral dimension along networks is quite small. A remarkable property of the NKp family of landscapes is the apparent invariance of the auto-correlation function with respect to the p parameter in the following sense: recall that the auto-correlation function $\rho_G(d)$ for a given fitness landscape G is not a statistical measure (Section 2). However, taking as a sample space all NKp landscapes G for fixed N , K and p we may consider the auto-correlation function as a continuous random variable, which we write as $\rho(d)$, or $\rho_{N,K,p}(d)$ if we wish to make the dependence on landscape parameters explicit.

Figure 3.1.5 plots $\langle \rho(d) \rangle$ [the mean of $\rho(d)$] for $N = 30$, $K=4$ and a range of p values. $\langle \rho(d) \rangle$ was estimated as follows: for each of a sample of 1000 landscapes, for each $d = 1$ to 15, a sample of 1000 pairs of genotypes Hamming distance d apart was taken to estimate $\rho(d)$ for that landscape. The result was then averaged over the sample of landscapes to obtain the mean. As can be seen, there is virtually no variation of $\langle \rho(d) \rangle$ with p - this was verified by a standard χ^2 test. The same result was obtained for a wide range of N , K , p and d values, including p very close to 1. So far an analytic proof has proved intractable (see also below), but there is sufficient confidence in the result to state it as a formal conjecture:

Conjecture 3.1.1

The mean (estimated value) $\langle \rho_{N,K,p}(d) \rangle$ of $\rho_{N,K,p}(d)$ as defined above is independent of p for $0 \leq p < 1$.

It is also worth remarking that the *variance* of $\rho_{N,K,p}(d)$ with respect to p is very low - i.e. $\langle \rho_{N,K,p}(d) \rangle$ provides an excellent estimate of $\rho_G(d)$ for any *particular* NKp landscape G , and indeed for a given NK landscape.

This result is at first sight paradoxical, as we would suspect that the expected high proportion of pairs of genotypes with equal fitness (particularly for $p \rightarrow 1$) would tend to produce higher correlation figures for increasing p . However, as remarked above, the landscape actually appears to become more rugged with increasing p and the effects seem to "cancel" each other. In fact what appears to happen is that the covariance of $f(g)$ with $f(g')$ for genotypes (g, g') Hamming distance d apart scales the same as the variance of $f(g)$ with respect to the p parameter for fixed N and K . This is made more precise in the following conjecture: let us define, for an NKp landscape G :

$$\text{cov}_G(d) \equiv \frac{1}{|G^{(d)}|} \sum_{(g, g') \in G^{(d)}} (f(g) - \bar{f})(f(g') - \bar{f})$$

where $G^{(d)} \equiv \{(g, g') \in G \times G \mid h(g, g') = d\}$ and $\bar{f} \equiv \frac{1}{|G|} \sum_{g \in G} f(g)$ is the landscape mean fitness.

Note that this is again not the usual statistical definition of covariance, but a unique number defined for a landscape G ; as for the auto-correlation function, however, we associate a random variable $\text{cov}(d) = \text{cov}_{N,K,p}(d)$ over the sample space of all NKp landscapes. Note that $\text{cov}_G(0)$ is simply the fitness variance $\sigma_f^2 \equiv \frac{1}{|G|} \sum_{g \in G} (f(g) - \bar{f})^2$.

Conjecture 3.1.2

For $d = 0, \dots, N$

$$\langle \text{cov}_{N,K,p}(d) \rangle = \phi_{N,K}(d)(1-p)(1+3p)$$

for some function $\phi_{N,K}(d)$ (which doesn't depend on p) and we have:

$$\langle \rho_{N,K,p}(d) \rangle = \frac{\phi_{N,K}(d)}{\phi_{N,K}(0)}$$

The second part of the conjecture follows from the definition of the auto-correlation function (Section 2.1). The formula was suggested by Conjecture 3.1.1 and a polynomial data fit.

Figure 3.1.6 plots $\langle \text{cov}_{N,K,p}(d) \rangle$ from sampled data and for the formula given in Conjecture 3.1.2 against p for $d = 0, \dots, 10$ for $N = 30$ and $K = 4$. Again a standard χ^2 test indicated an excellent fit. Note that the variance/covariance always peaks at $1/3$. Figure 3.1.7 plots the factor $\phi_{N,K}(d)$ for the same sample.

Finally, for a "degenerate" NKp landscape, where only one fitness table entry is non-zero, we can explicitly calculate the auto-correlation. The result (surprisingly, since there is no obvious reason to believe that such a landscape should yield values close to the statistical expectation) turns out to be an

extremely good fit for $\langle \rho_{N,K,p}(d) \rangle$, and we conjecture that this is indeed the case. The calculation is somewhat lengthy and can be found in Appendix A.2 - here we just quote the result:

Conjecture 3.1.3

For an NKp landscape (and hence an NK landscape, if Conjecture 3.1.1 holds), the (mean) auto-correlation function is given by:

$$\langle \rho_{N,K,p}(d) \rangle = \frac{(P-1)^2 \alpha(d) - 2(P-1)\beta(d) + \gamma(d)}{P(P-1) \binom{N}{d}}$$

where

$$\alpha(d) = \begin{cases} \binom{L}{d} & \text{if } d \leq L \\ 0 & \text{otherwise} \end{cases}$$

$$\beta(d) = \binom{N}{d} - \alpha(d)$$

$$\gamma(d) = (P-1) \binom{N}{d} - \sum_{\text{Max}(1,d-L) \leq k \leq \text{Min}(d,K+1)} \binom{K+1}{k} \binom{L}{d-k}$$

and we have set $P = 2^{K+1}$ and $L = N - K - 1$.

Figure 3.1.8 plots $\langle \rho_{N,K,p}(d) \rangle$ as calculated according to Conjecture 3.1.3 against sampled data for $N = 30$, $K = 0, \dots, 10$. The sampled data comprised 1000 pairs of genotypes for each of 1000 landscapes for each value of K . Again a χ^2 test indicated an excellent fit.

This concludes our analysis of NKp landscapes. As a test-bed for the study of population dynamics they provide an interesting family of landscapes for which the correlation structure and degree of neutrality may (if Conjecture 3.1.1 holds) be *independently* varied.

Finally, it is hoped that the conjectures in this sub-section may be proved analytically.

3.2 The RNN Family of Landscapes - Walking the Hypercube

The RNN landscapes were designed as a very basic general model of landscapes with neutral networks and hopefully to reflect some characteristics of RNA secondary structure folding landscapes. There are several reasons for wishing to construct simplified models for such landscapes. RNA folding landscapes provide one of the few examples where abstract landscape theory and computer simulations of population dynamics may be brought to bear on a "real biological" scenario, and one which is of great importance in molecular biology. One problem with the analysis of existing RNA folding landscape models, however, is the high computational cost of fitness evaluation - another is the sheer complexity of the folding algorithms (and hence of any secondary structure-based fitness function) [22]. These factors conspire against abstract analysis of the features of these landscapes

which may be relevant to their population dynamics. Thus it seems worthwhile to have available computationally cheaper and conceptually simpler models.

Previous work has applied random graph and percolation theory to the construction of landscapes with percolating neutral networks [21, 6, 20]. While these random graph landscapes appear to capture many of the structural characteristics of RNA folding landscapes, they do not seem to be very "tuneable" with regard to the dimension, size, number and degree of percolation of neutral networks. The RNN family of landscapes allow specification of these properties, although not quite independently. They also have some features in common with so-called "holey" landscapes [7, 8].

Again only binary genotypes are considered (although the construction generalises to arbitrary numbers of alleles). The actual construction is as follows: let N be the genotype length, and Q^N the binary N -hypercube. There are two parameters: a number $R > 0$ of neutral networks and a neutral dimension D where $1 \leq D \leq N$. The basic idea of the construction involves choosing R mutually disjoint $D-1$ dimensional (sub)hypercubes $H_r \subset Q^N$ for $r = 1, \dots, R$ with $H_r \cap H_\beta = \emptyset \quad \forall \alpha, \beta$. We then allow the R hypercubes to perform "simultaneous" mutually- and self-avoiding random walks in Q^N . This requires some clarification: a "step" on the random walk for a hypercube H consists of a parallel translation of H - all vertices of H step in the same direction. A hypercube of dimension $D-1$ in Q^N may be identified with a *schema* [11, 9] of order $N-D+1$; i.e. $N-D+1$ bits are defined - the vertices are represented by those bit-strings obtained by replacing the undefined positions of the schema by all possible combinations of 1's and 0's. Then a step is made by flipping one of the defined bits of the schema. E.g. if $H = 0*11**011*1*$ (here $N = 12$ and $D = 6$) we might flip bit 4 to get the new hypercube $H' = 0*10**011*1*$ which is then one step away from H . Figure 3.2.1 illustrates the process for $N = 3$, $D = 2$.

Evidently a $D-1$ dimensional hypercube has $N-D+1$ "degrees of freedom" to walk. The walks are performed "simultaneously" by randomly choosing a hypercube to walk at each step. The random walks continue until no further steps are possible for any of the hypercubes - i.e. Q^N has been "filled up" as far as possible by the walking hypercubes. To complete the construction, for each r we take the set of genotypes G_r traced out by the vertices of hypercube H_r and independently assign them a fitness f_r chosen randomly and uniformly in the range $[0,1]$. The remaining genotypes in Q^N are arbitrarily assigned a fitness of 0. The G_r 's (and the genotypes of zero fitness) thus become the neutral networks on our landscape.

The reason we work with $D-1$ rather than D , is that we would expect the mean neutral dimension (as defined in Section 2.2) of each neutral network G_r to be approximately D . It may, in fact, be either less than or greater than D : if a walk approaches within one mutation of *itself* additional neutral mutations will be introduced, raising the local neutral dimension. Random walk theory could perhaps be deployed to estimate how often this is likely to happen. On the other hand, the local neutral dimension at the "ends" of the random walks will be $D-1$. If a random walk is short its "ends" will contribute significantly to the mean neutral dimension - this is likely to happen if either R or D is large, in which case many random walks become quickly "boxed in". In practice the variance turns out to be fairly low. These effects can be observed in the neutral network statistics for $N = 18$ displayed overleaf in Figures 3.2.2a-d. Here $R = 100$ (figs. a and c), $R = 500$ (figs. b and d), $D = 4$ (figs. a and b) and $D = 8$ (figs. c and d). The data for each histogram represents an average over 10 RNN landscapes.

The percolation index is, as we might expect, comparatively high for small R . The neutral networks in this case are extremely "tangled" - every network has a good chance of coming within one mutation of every other. As we increase R the percolation index drops off, since on the one hand the size of the networks decreases, and in addition there are comparatively more neutral networks to get close to. Increasing D also decreases the size of the networks; furthermore the reduced "co-dimension" or number of "degrees of freedom" of the networks (given by $N-D$), restricts their ability to intertwine, and hence get close to each other - the networks are less "tangled" than for small D . [An attractive analogy is the fact that a length of string may be knotted in three, but not in two dimensions...]

The mean neutral dimension falls as R increases. This is due to the effects mentioned previously. The variance of neutral dimension along the networks is harder to fathom. In general we would expect the

variance to be high for small networks due to the "end effects". On the other hand large networks are likely to approach within one mutation of *themselves* quite frequently, thus also increasing the variance.

A related issue is to what extent Q^N is likely to be filled up before the walks grind to a halt. This would seem to be a difficult question to address analytically. There is also the practical possibility that the construction procedure falls at the first hurdle - it may be difficult (or impossible) to find any R hypercubes that are mutually disjoint for large R or D . Figure 3.2.3 plots the average fraction v of Q^N filled by genotypes of non-zero fitness for a range of R and D values for $N = 18$. Figures are averages over 10 landscapes. Gaps in the graph represent failure of the algorithm⁷ to place R initial hypercubes of dimension $D-1$. We see from the graph that the fraction v falls off quite sharply with increasing D and appears to asymptote at roughly $v = 0.2$. There is a slight increase in v with increasing R . Note that we would expect the mean neutral network size to be roughly $v \cdot \frac{2^N}{R}$. Comparing the **size** histograms of Figures 3.2.2a-d with v derived from Figure 3.2.3 indicates this to be a good approximation.

Finally, we examine the auto-correlation function for RNN landscapes. Figures 3.2.4a and b plot $\langle p(d) \rangle$ (estimated from a sample of 10,000 pairs of genotypes averaged over 25 RNN landscapes), for a selection of R and D values.

It is to be expected that the only correlation present in RNN landscapes will be the correlation of fitnesses between pairs of points on the *same* neutral networks (since the fitnesses of the neutral networks themselves are uniformly distributed and hence entirely uncorrelated). As R increases an arbitrarily chosen pair of genotypes a given Hamming distance apart are more and more likely to be on different neutral nets and their fitness thus uncorrelated. This effect is evident in Figure 3.2.4a. Conversely, as D increases genotypes close together in Hamming distance are increasingly likely to be on the same neutral network: consider the case $d = 1$. Here a 1-bit mutation has, on average, a probability of roughly $\frac{D}{N}$ of being neutral. A d -bit mutation thus has a probability of roughly $\left(\frac{D}{N}\right)^d$ of being neutral. Again, this trend is demonstrated in Figure 3.2.4b.

For larger Hamming distances ($d \gg D$) RNN landscapes are virtually uncorrelated. It must be remarked, however, that the auto-correlation function would seem to be of limited value on RNN landscapes (and to some extent on any landscape with extensive percolating neutral networks, particularly where the neutral dimension is high). For when there is a high degree of percolation then given a genotype, a neighbouring genotype will either lie on the same neutral network (and be completely correlated in fitness), or will belong to an *arbitrary* different neutral network (and thus be of uncorrelated fitness). In this context fitness correlation tends to be "all or nothing".

In the following Sections we shall see that on such landscapes the typical population dynamic is of such a nature as to render auto-correlation virtually irrelevant. For "intermediate" degrees of percolation the modified auto-correlation measure mooted in Section 2 may be more relevant to the dynamics.

⁷ The construction algorithm employed to collect sample data for this paper tries to place R randomly chosen hypercubes one at a time, discarding a choice if it intersects an already chosen hypercube. If at some stage it fails after 100- R attempts to place a hypercube the entire placement procedure restarts. After 10 restarts the construction algorithm times-out and gives up. Failure of this (rather crude) algorithm does not, of course, imply the impossibility of finding R disjoint hypercubes - nevertheless there will, it seems, be a point at which a "regular" (rather than random) arrangement of hypercubes will be enforced. The picture is not clear...

4 Population Dynamics

Up to this stage we have deliberately avoided use of the term "phenotype". The reason for this is simply that the concept does not enter into the formal definition of an abstract fitness landscape. In this section we do introduce the term for the principal reason that some standard terminology, particularly in the biological literature, is very often phrased in terms of "phenotype". In the context of fitness landscapes "phenotype" denotes an intermediate level of mapping between genotype and fitness value. Since our abstract landscapes do not (explicitly) involve such mappings, *the reader may substitute "fitness" for "phenotype"* wherever abstract landscapes, including the models introduced previously in Section 3, are discussed. A caveat is that, of course, the phenotype/fitness distinction cannot in general be ignored in the literature, so our use of the terminology must be viewed as specific to the abstract scenarios dealt with in this paper.

We start with some formal definitions regarding populations of genotypes. In the following let G be a fitness landscape of binary genotypes of sequence length N ; i.e. a mapping $f: Q^N \rightarrow \mathbf{R}$ where Q^N is the N -dimensional hypercube. As usual we identify G with the underlying set Q^N .

- (1) A (finite) **population** P on G is a mapping $P: G \rightarrow \mathbf{N}$ where \mathbf{N} is the set of integers 0, 1, 2, ... Intuitively $P(g)$ is the number of copies of g in P . [By abuse of notation we will sometimes write $g \in P$ to mean $P(g) > 0$, or we simply say " g is in P ".] The **size** of P is

$$|P| \equiv \sum_{g \in G} P(g)$$

- (2) The **genotypic support** of P is defined to be $\text{gsupp}(P) \equiv \{g \in G \mid P(g) > 0\}$ i.e. $\text{gsupp}(P)$ is the set of all genotypes with at least one copy in P .

- (3) The **phenotypic support** of P is defined as $\text{fsupp}(P) \equiv \{f \in \mathbf{R} \mid \exists g \in \text{gsupp}(P) \text{ s.t. } f(g) = f\}$ i.e. $\text{fsupp}(P)$ is the set of all fitness values represented by at least one genotype in P . The reader is reminded that we use the term "phenotype" and "fitness" interchangeably.

- (4) Given a fitness value f , define the population P^f to be the sub-population of P comprising all genotypes with fitness f ; i.e. $P^f(g) \equiv \begin{cases} P(g) & \text{if } f(g) = f \\ 0 & \text{otherwise} \end{cases}$

- (5) The **genotypic entropy** of P is $\text{gentropy}(P) \equiv - \sum_{g \in \text{gsupp}(P)} \frac{P(g)}{|P|} \log \frac{P(g)}{|P|}$. It represents

the degree to which the population is "spread" over the landscape. If the entire population were converged to a single genotype the genotypic entropy would yield zero. At the opposite extreme, if no two genotypes in the population were the same, it would attain its maximum of $\log(|P|)$.

- (6) The **phenotypic entropy** of P is $\text{fentropy}(P) \equiv - \sum_{f \in \text{fsupp}(P)} \frac{|P^f|}{|P|} \log \frac{|P^f|}{|P|}$. It represents the

degree to which the population is spread over the various fitness values. If the entire population had the same fitness the phenotypic entropy would be zero. It attains a maximum when the population is maximally spread over the possible fitness values. If $\text{fsupp}(P) < |P|$ this maximum will be $\log(|\text{fsupp}(P)|)$, otherwise it will be $\log(|P|)$.

- (7) The **dominant genotype** of P is the genotype g^* such that $P(g^*)$ attains a maximum over all possible genotypes⁸; i.e. g^* is the genotypes value with the most copies in the population.
- (8) The **dominant phenotype** of P is the fitness value f^* such that $|P^*|$ attains a maximum over all possible fitness values; i.e. f^* is the fitness value with the most representatives in the population. We will also write P^* to denote P^* i.e. the sub-population of P with fitness equal to the dominant phenotype. [See also the footnote to (7)].
- (9) The **centroid** of P is a real-valued N -dimensional vector $\mathbf{c} = \mathbf{c}_P \in \mathbf{R}^N$ defined by
- $$c_i \equiv \frac{1}{N} \sum_{g \in \text{gsupp}(P)} P(g) g_i \quad \text{where } g_i = 0 \text{ or } 1 \text{ is the allele of } g \text{ at locus } i. \mathbf{c} \text{ may be thought of as}$$
- the centre of mass of the population considered as a set of points (weighted by their multiplicity in the population) on the hypercube Q^N embedded in the vector space \mathbf{R}^N .
- (10) An **evolutionary algorithm** on G is a stochastic process associating a population P_t to each $t = 1, 2, 3, \dots$. Here t represents a (discrete) time parameter measured in **generations**. If $|P_1| = |P_2| = |P_3| = \dots = M$, say, then we say that algorithm has fixed population size M .

Before introducing the measures that will be used to gauge the dynamics of our evolutionary models, the evolutionary algorithm employed is described. We use a very simple tournament-based "fitness-proportional" genetic algorithm acting on a fixed population. The reasons we eschew more complex and possibly realistic models are twofold. Firstly there is enough complexity inherent in (and comparatively little solid theoretical basis for) the dynamics of even this very basic model; secondly much of the existing theory, particularly as regards evolution on the molecular level, is based on very similar models, or may be reviewed in similar terms. This includes various "quasispecies" [5, 2], "birth and death" [6] and "flow reactor" [13, 6] models and some common (haploid, asexual) models from population genetics [3]. The algorithm is as follows:

Given a fitness landscape G , a population P on G and a per-locus mutation rate m , we define a **tournament** to be a stochastic mapping of P to a new population P' defined as follows:

- (i) P' starts off as a copy of P .
- (ii) Two parent genotypes g_1, g_2 and an offspring genotype g_3 are chosen independently at random and with replacement from P' (thus some, or even all of the g 's may be the same genotype).
- (iii) One parent is selected from g_1, g_2 with probability proportional to their relative fitness; i.e. if the fitness of g_α is f_α for $\alpha = 1, 2$ then the probability that g_α is selected is $\frac{f_\alpha}{f_1 + f_2}$. A copy of the selected parent then replaces the offspring g_3 in P' . Note that a genotype may replace itself.
- (iv) Each locus of the replaced genotype g_3 is mutated (i.e. the bit at that locus is flipped) independently with probability m .

Note that the size of the population P' remains unchanged at M . We now define an evolutionary algorithm P_t iteratively by choosing P_{t+1} to be the population obtained from P_t by iterating the above tournament mapping M times⁹.

⁸ By this definition g^* will not be unique if more than one genotype in the population shares the maximal number of copies. In practice for reasonably large populations this is extremely unlikely, so we conveniently ignore the possibility.

⁹ It can be shown that this scheme is similar to Roulette Wheel selection from, and replacement of, the entire population at each generation. A difference lies in the variance of the distribution of number of offspring per genotype, although the mean (expectation) is the same.

With *finite* populations evolutionary dynamics must be considered as a stochastic process [4, 18]. Due to the huge number of degrees of freedom present in any reasonably sized population we are forced to seek statistical quantities in order to characterise the dynamics. Below we shall motivate and describe the statistical measures used in this paper. First, however, we digress to discuss a particular aspect of population dynamics often encountered in the literature, that of a "wild-type" or "master" genotype [5, 18]. The idea, it seems, is intimately connected with a single-peaked fitness landscape (or at best a converged population in the locality of a single peak of a multi-peaked landscape). On such landscapes it is observed and may be analytically verified [25], that (for low mutation rates) populations tend to cluster around a predominant "master" genotype of (locally) optimum fitness¹⁰. Selection will tend to reproduce the optimum genotype preferentially, thus maintaining its predominance. As the mutation rate is increased the population is able to maintain a higher proportion of genotypes at small (Hamming) distances from the optimum genotype, so that the population forms a "cloud" around the optimum. At some critical mutation rate, the *genotypic error threshold*, selection is no longer able to maintain the optimum genotype, which disappears from the population. The phenomenon known as *Muller's Ratchet* sets in, whereby mutation drives the population from the optimum more strongly than selection can restore it¹¹. The population now forms a cloud *around* the fitness peak. Beyond some still higher critical mutation rate, which we term the **information error threshold** the population (still in the form of a "cloud", due to the effects of random drift in a finite population) wanders randomly around the landscape, all information about the whereabouts of the peak having been lost¹². This process is now quite well understood, and accurate estimates exist for values of the genotypic error threshold, at least on simple landscapes [18, 25]. It should also be stressed that the genotypic error threshold is not a property of a fitness landscape *per se*, but rather of a landscape's structure in the neighbourhood of a peak.

The problem with this scenario (and certainly with the existing analysis) is that it does not carry over to the situation of large-scale neutrality. If the local optimum fitness is no longer a peak but a "ridge" or neutral network of equally fit one-mutant neighbours there is no longer a single "master" genotype. Selection acts equally on all genotypes belonging to the neutral network. There is a sense, however, in which the genotypes on the locally optimum neutral network collectively represent a "master" entity of sorts. In the literature they are sometimes referred to as the "master" or "dominant" phenotype, although this term may, in fact, refer to an actual phenotype (c.f. the discussion at the beginning of this Section). By abuse of terminology we shall refer to the "dominant phenotype" of the current population as defined at the start of this Section, bearing in mind that for our purposes phenotype \equiv fitness¹³. We will also refer to the "dominant *neutral network*" associated with the dominant phenotype.

The nearest analogue to the single-peaked landscape is a "single ridge" landscape; i.e. there is a single neutral network of optimum fitness, the remainder of the landscape being genotypes (possibly forming other neutral networks) of lower fitness. The following scenario then pertains: at low mutation rates the population drifts as a cloud on the optimum neutral network (corresponding to the dominant phenotype). The rate of drift, or *diffusion* has been calculated explicitly for a *flat* landscape [4]. As the mutation rate increases the population maintains a small proportion of genotypes which do not lie on the neutral network - the cloud "overlaps" the neutral network. There is then a critical mutation rate, the *phenotypic error threshold* [6, 13] at which selective pressure can no longer hold the bulk of the population on the dominant phenotype, and the population forms a cloud around the dominant phenotype. This threshold may be accurately estimated for some simple landscapes [6]. A difference

¹⁰ The term "master genotype" is sometimes used to refer to a population "consensus sequence", which is the genotype nearest the centroid in \mathbf{R}^N . This genotype may well not, in fact, actually exist in the population. The discussion which follows does not apply to this usage of the term.

¹¹ Strictly speaking Muller's Ratchet considers very long sequence length genotypes and ignores the possibility of "back mutation", so that the population is driven inexorably away from the optimum genotype. With finite populations and/or shorter genotype lengths the possibility of back mutation cannot be entirely ignored. See [24] for details.

¹² In "needle in a haystack" models, where the single peak sits in an otherwise flat landscape, the information error threshold will coincide with the genotypic error threshold, since loss of the "needle" from the population implies loss of all information as to its whereabouts.

¹³ The "master" or "dominant" phenotype terminology seems to have arisen from the literature on RNA structure evolution, where the fitness of a genotype is commonly (and often implicitly) defined as the "distance" of the secondary structure (\equiv phenotype) from a pre-specified "master" structure [13]. Thus many phenotypes can map to the same fitness value - however the "master phenotype" will still correspond to our "dominant phenotype" presuming that structures at distance zero must coincide.

from the peaked landscape scenario is that the phenotypic error threshold, rather than being a property of the landscape structure in the neighbourhood of the entire dominant neutral network, may be dependent on the *particular neighbourhood of the population* on the dominant neutral network. This phenomenon is crucial to understanding the dynamics of populations which we shall observe in simulations in the next Section. At a high enough mutation rate an information error threshold is encountered and the population is unable to remain in the locality of any dominant phenotype at all, drifting randomly around the landscape. Unlike the peaked landscape case, the phenotypic error threshold is likely to be "fuzzy" due to its dependence on the particular locality on the dominant neutral network that the population finds itself on. The information error threshold, on the other hand, appears to be a property of the *gross* structure of the landscape.

The statistical measures we employ are designed to reflect the dynamical description given above. In particular, we want to be able to measure the degree to which the population is spread out - the size of the "cloud" - and the rate at which the cloud is "drifting". We also want to be able to detect the onset of the error thresholds. Most measures are time-dependent; i.e. they are associated with the population P_t at a given generation t . They may be averaged over an evolutionary run and possibly over a sequence of runs. We divide them into five categories:

I. Fitness Measures

In this category we monitor the current population mean fitness and highest fitness, and the fitness value of the dominant phenotype. The latter should enable us to identify which neutral network the population is currently clustered around; for very high mutation rates it may fluctuate wildly, as the population is likely to be spread more or less randomly over all neutral networks. Fluctuation of the dominant phenotype as we have defined it is thus an indicator of proximity to a phenotypic error threshold.

II. Phenotypic Error Measures

We define the **phenotypic error** at generation t to be $1 - \frac{|P_t^*|}{M}$. This is the proportion of genotypes in the population which do not represent the dominant phenotype; i.e. are not on the neutral network associated with the dominant phenotype. It lies between 0 and 1. Again, a high value ($>> 0$) for the phenotypic error suggests that we are close to a phenotypic error threshold.

We define the **phenotypic loss** to be the number of times up to the current generation that the dominant phenotype fell in value. We also define the **phenotypic loss rate** to be the number of times *per generation* that the dominant phenotype falls in value. It lies between 0 and $\frac{1}{2}$ but will generally be close to zero. It is also useful in detecting error thresholds. Caution must however be exercised in drawing conclusions from this measure, as its variance (over the course of a run) tends to be high. In practice it must be averaged over many (and/or very long) runs.

III. Entropic measures

The **genotypic entropy** has been defined at the start of this Section. While it is perhaps more common to use the average Hamming distance between genotypes to measure how "spread out" a population is, entropy measures rather the amount of "disorder" in the distribution of genotypes among the population. In practice it often correlates quite closely with average Hamming distance and is comparatively cheap in computational terms.

The **phenotypic entropy** measures how spread out the population is over the possible fitness values, or, equivalently, over the neutral networks. In practice it tends to correlate quite closely with the phenotypic error (see II above).

IV. Diffusion measures

The *diffusion coefficient* is defined as the square of the (Euclidean) distance (in \mathbf{R}^N) travelled by the population centroid $\mathbf{c}(t)$ per generation. It measures the rate at which the population "cloud" drifts through the fitness landscape. In practice this quantity tends to fluctuate quite rapidly from generation to generation and is more fruitfully presented as an average over several generations. In the results presented in the next section we calculate a "rolling" average of the diffusion coefficient over the last 100 generations to smooth it out. For flat fitness landscapes the expected value of the diffusion constant may be estimated [4, 13]. For binary genotypes the calculation for a flat landscape yields¹⁴:

Eq 4.1
$$D_0 = \frac{Nmr}{1 + 2Mm}$$

where N = genotype sequence length, m = per-locus mutation rate, M = population size and r is the "replication rate", given by the expected number of offspring per genotype per generation (which will be 1 in our case). This estimate is quite accurate, even for fairly high mutation rates. It is also stated in [13] that for a non-flat landscape with neutrality the diffusion coefficient may be approximated for low mutation rates by $D = \lambda D_0$ where λ is the mean fraction of neutral mutations [in our terminology $\lambda = (\text{neutral dimension} + 1)/N$]. This gives in our case:

Eq 4.1a
$$D = \frac{(v + 1)mr}{1 + 2Mm}$$

where v = (local) neutral dimension (which we calculate as an average over P^*). A heuristic argument for this value is as follows: if Eq 4.1 represents a population drifting on a flat landscape we can, for low mutation rates (where most of the population is confined to the neutral network of the dominant phenotype), view our situation as a population of genotypes of sequence length $(v + 1)$ drifting on a "flat" landscape, since only mutations which keep us "on the neutral network" are significant as regards drift. A plausible refinement of Eq 4.1a is derived by replacing M with the size of the population actually on the dominant neutral network; i.e. $|P^*|$. This yields:

Eq 4.1b
$$\tilde{D} = \frac{(v + 1)mr}{1 + 2|P^*|m}$$

We refer to D_0 as the "flat", D as the "unadjusted theoretical" and \tilde{D} as the "adjusted theoretical" diffusion coefficient. In our simulations in the next section we compute these quantities alongside the actual diffusion coefficient for comparison.

While the diffusion rate tells us about how "fast" the population is wandering about the landscape it does not actually tell us very much about how far it is wandering. For instance, on a single peaked landscape at a mutation rate higher than the genotypic error threshold (but not so high as to induce random drift of the population as a whole) the population centroid may move quite rapidly, but remain in the locality of the dominant genotype. We will be especially interested in the actual distances travelled by the centroid when comparing population dynamics on low and high neutrality landscapes and thus have need for a reliable measure of actual distances travelled by the centroid. To this end we also compute a "time-lagged" diffusion coefficient, which we define to be the square of the distance between the centroid "now" and its position t_{lag} generations previously, where we usually take $t_{\text{lag}} = 100$.

¹⁴ The formula given in [13] is for RNA sequences which have four possible allelic values (it also contains an error - the 5 should be replaced by a 6), and must be adjusted for the binary case. Furthermore, their definition of the centroid works out at twice the magnitude of that given in this paper for the binary case, so we must divide their diffusion coefficient by 2.

IV. Visualisation Techniques

Finally, to help us get an intuitive picture of the dynamical behaviour of the population on the fitness landscape we employ two visualisation techniques based on Principal Components Analysis (PCA) [14].

Firstly we wish to visualise the movement of the population centroid around the landscape. To this end we perform a PCA of the set of successive position vectors of the centroid and display the first two PC's as a 2-dimensional plot.

Secondly we wish to visualise the configuration of the "cloud" of genotypes representing a converged population. Here we use a technique from Distance Geometry [10] as described in [13]; for each generation t the matrix $m_{\alpha\beta} \equiv \frac{1}{2} (d_{0\alpha}^2 + d_{0\beta}^2 - d_{\alpha\beta}^2)$ is calculated, where $d_{\alpha\beta}$ is the Hamming distance between genotypes g_α and g_β for each $g_\alpha \in \text{gsupp}(P_t)$ and $d_{0\alpha}$ is the distance from g_α to the centroid $c(t)$. The first two eigenvectors of the matrix $m_{\alpha\beta}$, viewed as vectors in \mathbf{R}^2 , then capture most of the positional variation in the configuration of g_α 's (considered as vectors in \mathbf{R}^N). See [10] for a theoretical justification of this method.

In the next Section we apply our statistical analysis tools to GA simulations on RNN and NKp landscapes. We start with RNN landscapes, as they better illustrate the general principles.

5 Simulation Results

5.1 Population Dynamics on RNN Landscapes

Figure 5.1.1 displays the dynamics over 3000 generations of a simulation on an RNN landscape with $N = 20$, $R = 100$, $D = 6$. The population size is 1000 and the mutation rate 0.001. The initial population consisted of 1000 identical genotypes of fitness zero (note that on this landscape about 75% of all genotypes have zero fitness). Diffusion coefficients are rolling averages over the previous 100 generations. Average figures quoted are means over the last 2500 generations, to allow the dynamics to stabilise.

We see that the population steps up to successively higher fitness levels, represented by the current dominant neutral network. The phenotypic error is low (less than 5% on average) except where the population steps up to a higher network, indicating that the population is largely confined to the current dominant neutral network. The low phenotypic entropy (which tracks the phenotypic error closely) supports this conclusion, while the significant genotypic entropy (average ≈ 2.5 , possible maximum $\log_e 1000 \approx 6.9$) suggests that the population does indeed form a "cloud" on the neutral network. The overall picture strongly supports the scenario described in the previous section. We note that at this low mutation rate the population does not "slip off" a neutral network once attained - indeed the phenotypic loss rate (not displayed) is always zero - no phenotypic error thresholds are breached. An intriguing feature evident in this run is that after attaining the last neutral network (around generation 1200) there is a trend towards regions of higher neutral dimension. This phenomenon was frequently (but not invariably) observed for a range of mutation rates. The drifting population seems to "seek out" regions of comparatively high neutrality on its current neutral network. Note that this cannot be due to any relationship between fitness and network structure, as the fitness of a neutral network in an RNN landscape is randomly assigned. Finally the actual and theoretical diffusion coefficients are plotted. In this run the unadjusted theoretical coefficient (ave. 0.00252) is, on average, slightly better than the adjusted (ave. 0.00261); both approximate the actual coefficient (ave. 0.00251) well, particularly given the substantial variance of the actual coefficient.

Figure 5.1.2 displays the dynamics of a run on the same landscape with identical parameters, except that the mutation rate is now ten times higher, at 0.01. We see a notable difference in the dynamics.

The population still sporadically steps up to a higher neutral network, *but cannot generally sustain itself there for long* and slips again to a lower network. The phenotypic error is much higher, averaging about 44%, suggesting that somewhat over half the population is resident on the dominant neutral network at any one time; this is reflected in the phenotypic entropy. The genotypic entropy is also high, suggesting a much more diffused "cloud". An explanation for the overall behaviour is as follows: on attaining a higher neutral network, the population drifts on the network until it reaches a region of the network where the phenotypic error threshold *drops below the value of the mutation rate* (c.f. the discussion in Section 4). The population then slips to a lower network where it drifts until either slipping again, or encountering a region where selective pressure is again able to hoist it to a higher network. At about generation 1350 the population attains a neutral network which it appears to be able to sustain, at least for the remaining duration of the simulation. Note that this is not the highest network attained during the run. Thus we see that *the phenotypic error threshold varies among and within neutral networks*. The phenotypic loss rate was an average of 0.0068 episodes of phenotypic loss per generation. Again the population seems to "prefer" regions of higher neutral dimension. In this run the adjusted diffusion coefficient (ave. 0.0070) gives a significantly better estimate of the actual diffusion coefficient (ave. 0.0065) than the unadjusted (ave. 0.0038); it can be seen to "track" the actual coefficient to some extent.

In Figure 5.1.3 the mutation rate has been raised to 0.02. Again a qualitative difference is apparent. The population is even less able to sustain itself on high fitness neutral networks. Furthermore, when it slips off a network the population occasionally loses track of the "higher ground" entirely, and drifts at random among the ~75% of genotypes of fitness zero (which themselves constitute a neutral network); we are approaching the *information error threshold*. The phenotypic error is high, falling slightly when the population attains a (non-zero-fitness) neutral network. The genotypic entropy is near the maximum, suggesting that almost every genotype in the population is different. The neutral dimension graph reflects the dimension of the zero-fitness network (about 15) during the episodes of random drift. The theoretically calculated diffusion coefficients are now poor predictors of the actual diffusion coefficient, which is closer to the flat landscape rate - the neutral networks have almost relinquished their influence over the rate of diffusion.

At still higher mutation rates, beyond the information error threshold (results not included), the population drifts randomly about the landscape, unable to attain any higher neutral networks even momentarily. The population carries no information about the landscape structure. The diffusion coefficient is that of a flat landscape.

Figure 5.1.4 presents a statistical analysis of the dependence of the various dynamical measures on the mutation rate. Figures are averages over sets of 20 runs of 5000 generations each, on different randomly generated RNN landscapes. Population size is 1000 genotypes initially placed at random and averages are calculated starting at generation 500 to limit the influence of initial transients. The data supports our general thesis. There is no clearly defined phenotypic error threshold, although the average phenotypic error peaks at about $m = 0.026$, as does the phenotypic loss rate. This mutation rate could be described as the "mean phenotypic error threshold". The loss rate then drops to zero at about $m = 0.036$ as the zero-fitness neutral network becomes completely dominant. The phenotypic entropy peaks at the same value. We might thus describe $m = 0.036$ as the "mean information error threshold". The genotypic entropy asymptotes at its maximum of $\log_e 1000 \approx 6.9$. We see that the adjusted theoretical diffusion coefficient yields a good approximation to the actual coefficient for low mutation rates (up to about $m = 0.12$).

Finally, Figure 5.1.5 illustrates the trajectory of the centroid of a population of 1500 genotypes evolving on an RNN landscape ($N = 20$, $R = 100$, $D = 10$) over 2500 generations, while Figure 5.1.6 is a "snapshot" of the genotypic support for the same run. This Figure is comparable with Fig. 2 in [13] for a population evolving on an RNA folding landscape¹⁵, revealing similar clustering (as predicted in [4] for flat landscapes). Overall, the dynamics exhibit striking similarities to those described in [13] for RNA structure landscapes based on a folding algorithm.

¹⁵ Note that the colour key in our Figure 5.1.6 is not the same as in Fig. 2 in [13].

5.2 Population Dynamics on NKp Landscapes

Figure 5.2.1 presents the dynamics of a simulation run on an NKp landscape with $N = 20$, $K = 4$, $p = 0$ and mutation rate 0.001. All other details are the same as in Section 5.1. Figure 5.2.2 illustrates an identical run but with $p = 0.99$. Recall from Section 3.1 that these landscapes will have virtually identical auto-correlation functions.

The $p = 0$ case is a conventional NK landscape - multi-peaked and somewhat rugged (at $K = 4$). It is apparent from the fitness plot that the population engages in successive sojourns on local optima, punctuated by hill-climbs to higher optima. There are a few isolated instances where the population falls off a peak, but only momentarily, as we are well below the (genotypic) error threshold for at least "most" optima. The phenotypic error is generally high - on this landscape phenotype \equiv genotype since every genotype has (almost surely) a unique fitness value - so the phenotypic error here represents the fraction of the population different from the dominant *genotype*. Similarly, the phenotypic and genotypic entropies coincide. The neutral dimension (not plotted) is, of course, -1 as there is no neutrality. The theoretical estimates for the diffusion coefficient (not plotted) are, for the same reason, of no use.

For $p = 0.99$ the dynamics are distinctly different. We now have neutral networks, and the picture is not unlike the dynamics on RNN landscapes as seen in Section 5.1. A point of interest is that (unlike RNN landscapes) the neutral dimension may be observed to fall as the population climbs to higher neutral networks. This effect is explained by our analysis in Section 3.1, where we noted that neutral dimension falls as we move higher on an NKp landscape. The theoretical values for the diffusion coefficients now provide quite accurate estimates for the actual value. Overall, the picture is strikingly reminiscent of the RNN run of Figure 5.1.1 (particularly in the latter half of the run, where the neutral dimension is about 7) and quite unlike the $p = 0$ (NK) case.

Another difference is apparent from Figure 5.2.3 where we plot the *lagged* diffusion coefficient (with $t_{\text{lag}} = 100$) for the two runs. Recall that this represents the (squared) *distance* the population centroid moves (rather than its rate), here over 100 generations. Values are rolling averages, also over 100 generations. Peaks in the graphs represent episodes where the population is climbing to a higher hilltop ($p = 0$) or a higher neutral network ($p = 0.99$). We observe that *between* peaks the population on the $p = 0$ landscape does not travel very far - it remains in the locality of the current dominant genotype - while for the $p = 0.99$ landscape the population drifts appreciable distances along the dominant neutral network.

Similar runs for different values of K (which alters the correlation) point to the conclusion that in the presence of percolating neutral networks a landscape's *correlation* structure is a lesser determining factor of population dynamics than its *neutral* structure.

6 Conclusions

The NKp family of landscapes demonstrates that the correlation structure of a landscape can be of lesser significance than its neutral structure as regards evolutionary dynamics. NKp landscapes also illustrate that correlation can be deceptive and counter-intuitive in the presence of percolating neutral networks. Analysis and empirical results on the invariance of the auto-correlation function with regard to the p parameter also have potentially important implications for (the special case of) NK landscapes - it is to be hoped that the Conjectures in Section 3.1 may yield to theoretical analysis.

RNN landscapes provide a flexible and conceptually simple model for the analysis of neutral networks in general. It is suggested that they may also be a viable model for the study of evolutionary dynamics on RNA folding landscapes. The model could easily be extended to more than two alleles and to specifiable distributions of network size, number and dimension. Because of its relative simplicity population dynamics could perhaps also be analysed using techniques from statistical mechanics as in [17].

The analytic techniques introduced for landscape structure and population dynamics have proven useful in interpreting simulation results, although more work needs to be done in developing a dynamically meaningful measure of correlation for landscapes with neutrality. Simulation results suggest that the theoretical (adjusted) diffusion coefficient (Eq 4.1b) could be used (for low mutation rates) to estimate the local neutral dimension of neutral networks on landscapes of unknown structure. Future work, perhaps along the lines of [4], is required to extend its usefulness to higher mutation rates. More work is also required to extend the known results on (phenotypic) error thresholds [6] to more general landscapes. Knowledge of diffusion rates and error thresholds would be of great importance for the application of evolutionary techniques in optimisation problems to landscapes with neutrality. Together they could help predict optimum values for mutation rates, population size, etc. to maximise search effectiveness by exploiting neutral drift.

The phenomenon observed in Section 5.1, where evolving populations appear to seek out regions of high neutrality on a neutral network, also begs investigation - the biological implications are particularly intriguing.

Finally, the omissions listed in the Introduction need addressing, in particular the effects of noise, recombination and different selection schemes.

Acknowledgements

The author would like to thank Inman Harvey for his direction and encouragement and David Harper for helpful discussions on statistical procedures.

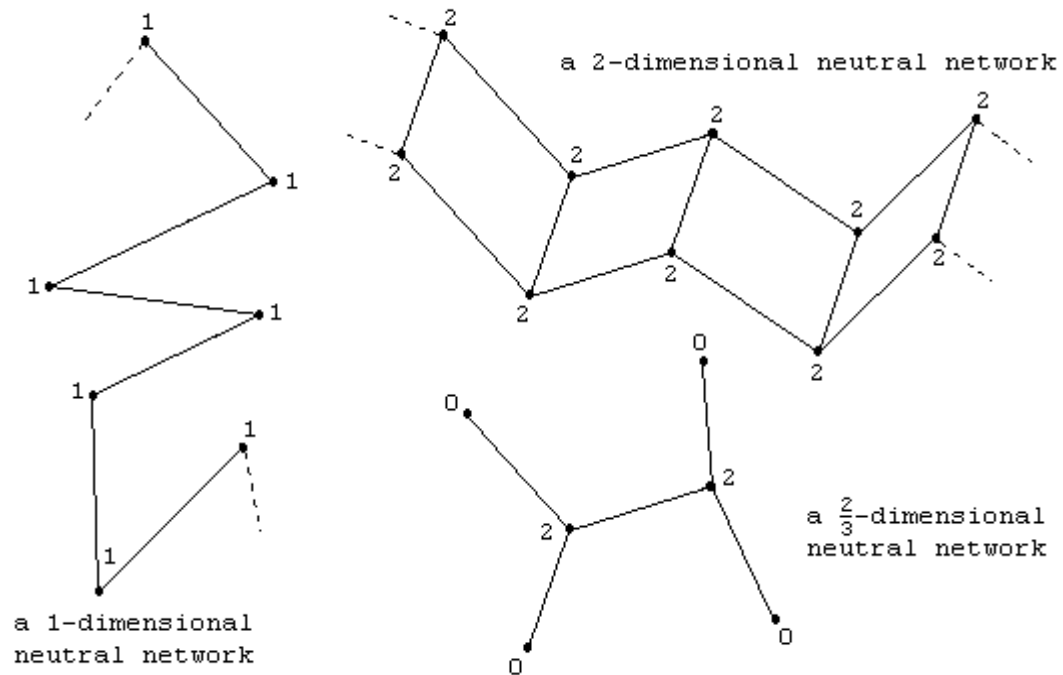
Lionel Barnett,

August 1997.

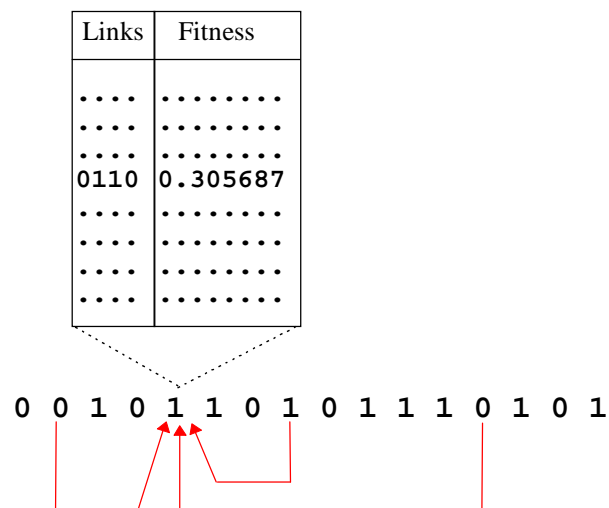
References

- [1] Baskaran, S., Stadler, P.F. & Schuster, P. (1995). *Approximate Scaling Properties of RNA Free Energy Landscapes*. Santa Fe Institute Preprint 95-10-083, Santa Fe, NM, USA.
- [2] Bonhoeffer, S. & Stadler, P.F. (1993). *Error Thresholds on Complex Landscapes*. J. Theor. Biol. **164**:359-372.
- [3] Crow, J.F. & Kimura, M. (1970). *An Introduction to Population Genetics Theory*. Harper & Row, New York.
- [4] Derrida, B. & Peliti, L. (1991). *Evolution in a Flat Landscape*. Bull. Math. Biol. **53**:355-382.
- [5] Eigen, M., McCaskill, J. & Schuster, P. (1989). *The Molecular Quasispecies*. Adv. Chem. Phys. **75**:149-263.
- [6] Forst, C.V., Reidys, C. & Weber, J. (1995). *Neutral Networks as Model-Landscapes for RNA Secondary-Structure Folding-Landscapes*. Lecture Notes in Artificial Intelligence, vol. 929: Advances in Artificial Life (Morán, F., Moreno, A., Merelo, J.J. & Chacón eds.), Springer-Verlag, Berlin.
- [7] Gavrillets, S. (1997). *Evolution and Speciation on Holey Adaptive Landscapes*. TREE vol. 12 (Elsevier Science Ltd.)
- [8] Gavrillets, S. & Gravner, J. (1996). *Percolation on the Fitness Hypercube and the Evolution of Reproductive Isolation*. J. Theor. Biol. **184**:51-64
- [9] Goldberg, D.E. (1989). *Genetic Algorithms in Search, Optimization and Machine Learning*. Addison-Wesley.
- [10] Havel, T.F., Kuntz, I.D., & Crippen, G.M. (1983). *The Theory and Practice of Distance Geometry*. Bull. Math. Biol. **45**:665-720.
- [11] Holland, J.H. (1975). *Adaptation in Natural and Artificial Systems*. MIT Press, USA.
- [12] Huynen, M.A (1995). *Exploring Phenotype Space through Neutral Evolution*. Santa Fe Institute Preprint 95-10-100, Santa Fe, NM, USA.
- [13] Huynen, M.A., Stadler, P.F. & Fontana, W. (1996). *Smoothness Within Ruggedness: The Role of Neutrality in Adaptation*. Proc. Natl. Acad. Sci. (USA) **93**:397-401.
- [14] Jain, A.K. & Dubes, R.C. (1988). *Algorithms for Clustering Data*. Prentice-Hall, New Jersey.
- [15] Kauffman, S. A., (1993). *The Origins of Order - Self-Organization and Selection in Evolution*. Oxford University Press, New York.
- [16] Kimura, M. (1983). *The Neutral Theory of Molecular Evolution*. Cambridge University Press, Cambridge, UK.
- [17] van Nimwegen, E., Crutchfield, J.P. & Mitchell, M. (1997). *Statistical Dynamics of the Royal Road Genetic Algorithm*. Santa Fe Institute Preprint 97-04-035, Santa Fe, NM, USA.
- [18] Nowak, M. & Schuster, P. (1989). *Error Thresholds of Replication in Finite Populations - Mutation Frequencies and the Onset of Muller's Ratchet*. J. Theor. Biol. **137**:375-395.

- [19] Press, W.H., Teukolsky, S.A., Vetterling, W.T. & Flannery, B.P. (1992). *Numerical Recipes in C - The Art of Scientific Computing*. Cambridge University Press, Cambridge, UK.
- [20] Reidys, C.M. & Fraser S.M. (1995). *Evolution on Random Structures*. Santa Fe Institute Preprint 95-11-087, Santa Fe, NM, USA
- [21] Reidys, C.M., Stadler, P.F. & Schuster, P. (1995). *Generic Properties of Combinatory Maps - Neutral Networks of RNA Secondary Structures*. Santa Fe Institute Preprint 95-07-058, Santa Fe, NM, USA
- [22] Schuster, P., Fontana, W., Stadler, P.F. & Hofacker, I.L. (1994). *From Sequences to Shapes and Back - A Case Study in RNA Secondary Structures*. Proc. Roy. Soc. (London)B, **255**:279-284.
- [23] Stadler, P.F. (1995). *Landscapes and their Correlation Functions*. Santa Fe Institute Preprint 95-07-067, Santa Fe, NM, USA
- [24] Weinberger, E.D. (1990) *Correlated and Uncorrelated Fitness Landscapes and How to Tell the Difference* Biol. Cybern. **63**:325-336
- [25] Woodcock, G. & Higgs, P.G. (1995) *Population Evolution in a Single Peak Fitness Landscape - How High are the Clouds?* Lecture Notes in Artificial Intelligence, vol. 929: Advances in Artificial Life (Morán, F., Moreno, A., Merelo, J.J. & Chacón eds.) p148-157, Springer-Verlag, Berlin.

**Figure 2.1.1**

Schematic diagram illustrating neutral dimension of neutral networks. Dots represent genotypes, labelled with their neutral dimension. Lines represent neutral mutations.

**Figure 3.1.1**

Schematic construction of an NK landscape, illustrating epistatic links (red arrows) and the fitness table associated with a locus.

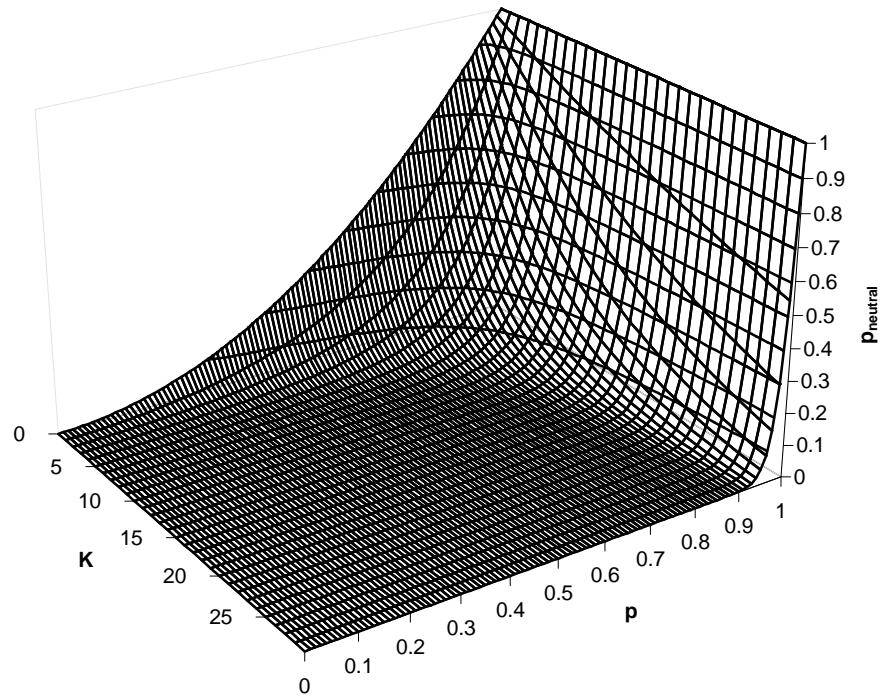


Figure 3.1.2

Calculated probability of neutral mutation in NKp landscapes for $N = 30$.

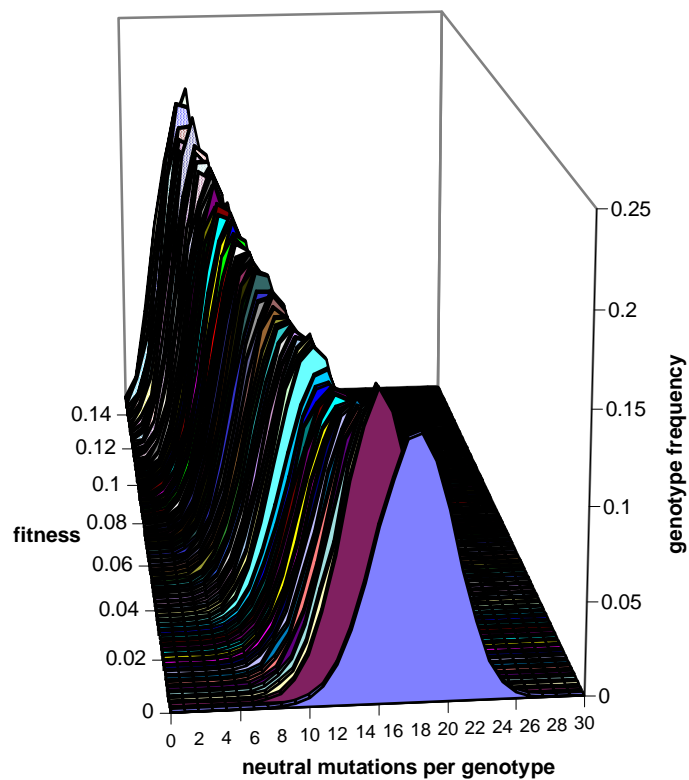
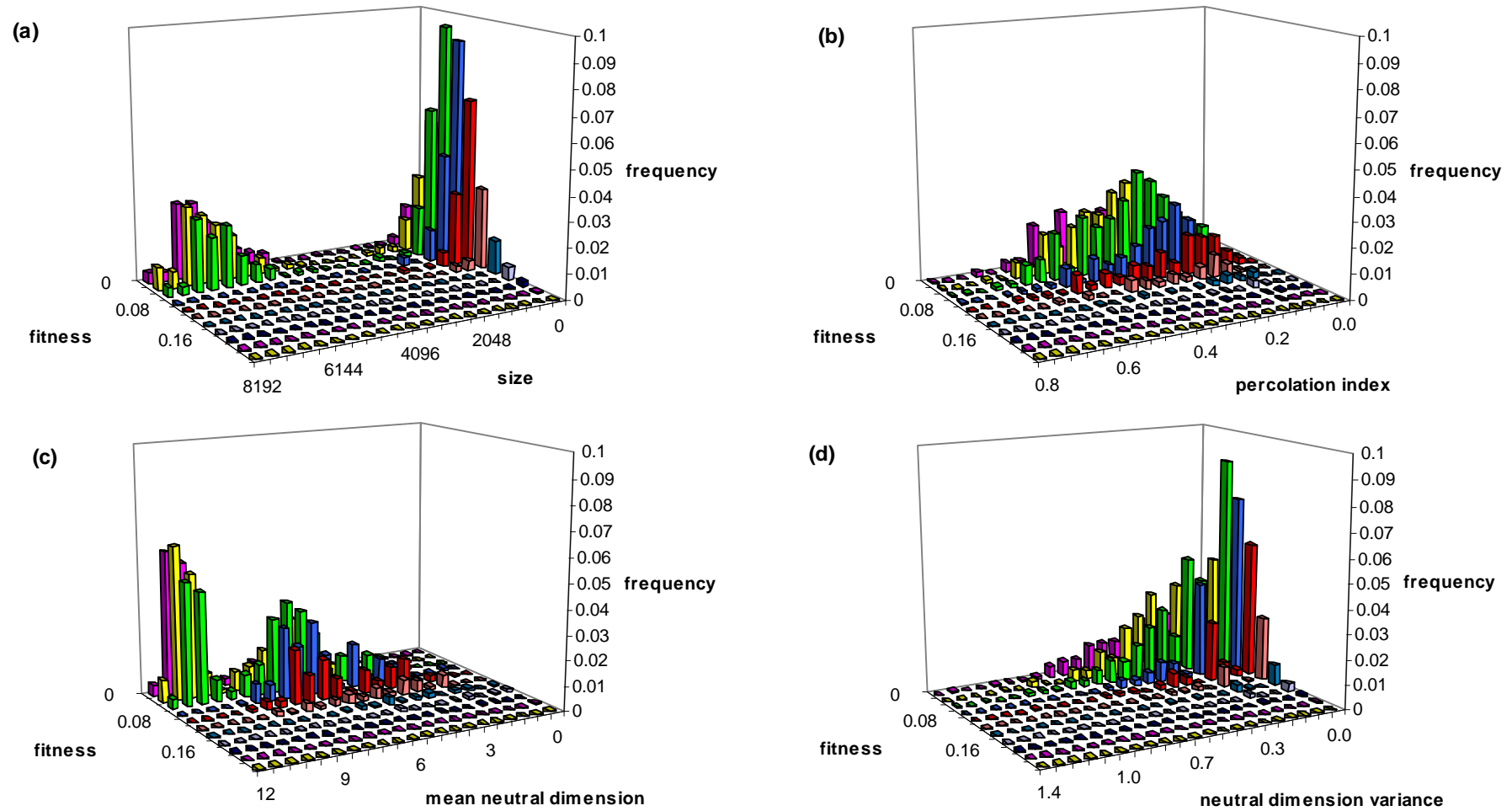
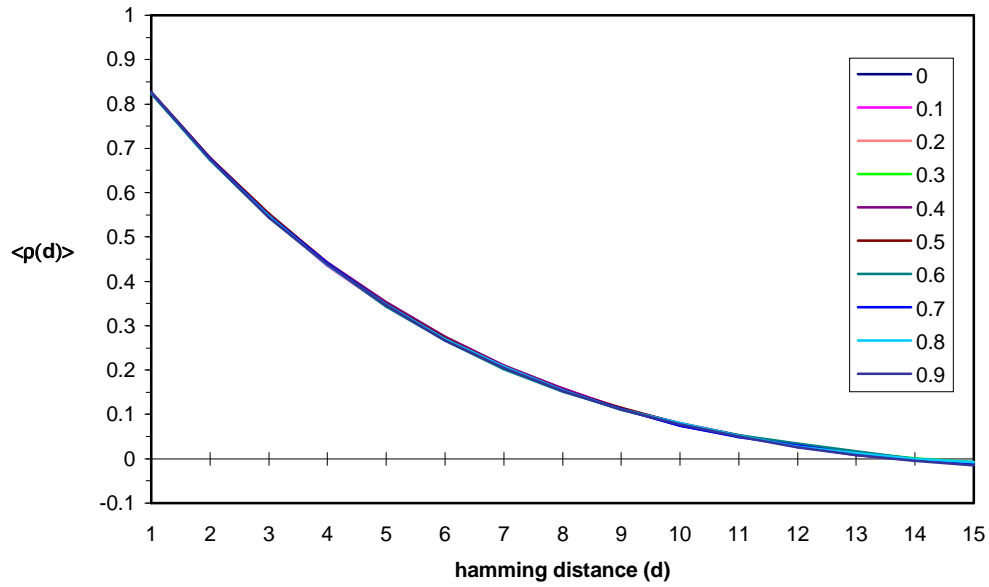


Figure 3.1.3

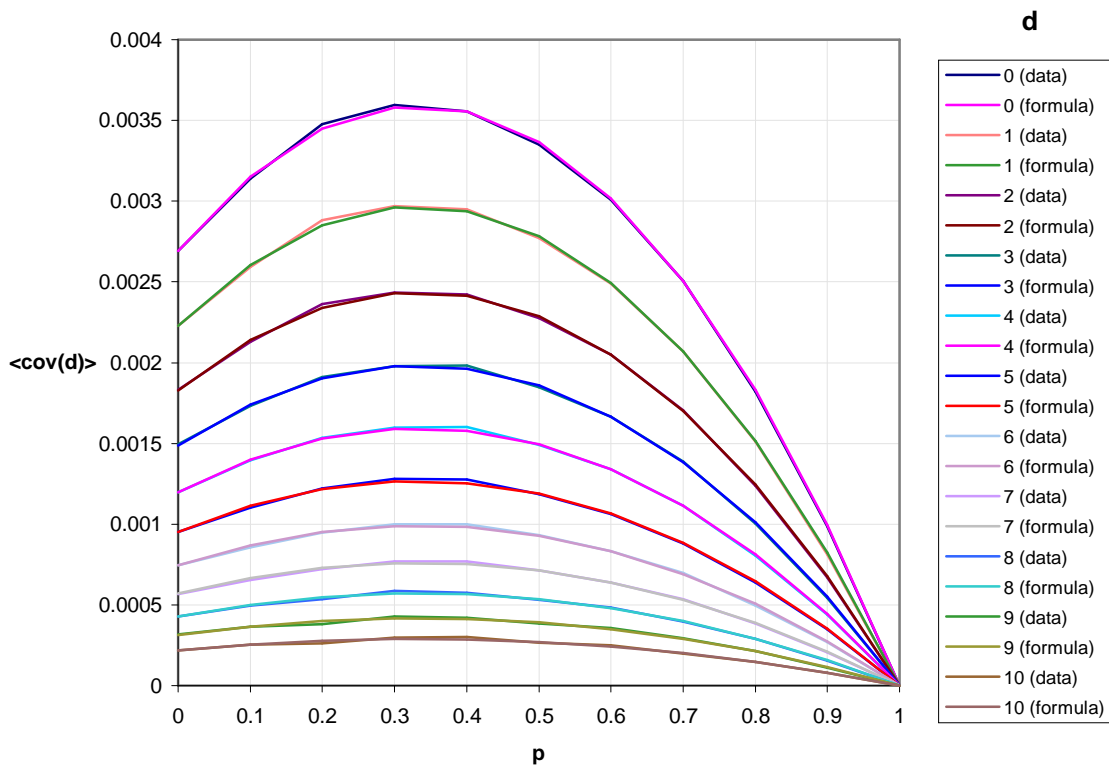
Distributions of neutral mutation for varying fitness in NKp landscapes ($N = 30$, $K = 4$, $p = 0.9$)

**Figure 3.1.4a-d**

Distribution of (non-zero fitness) neutral network statistics by fitness on NKp landscapes for $N = 18$, $K = 4$ and $p = 0.99$

**Figure 3.1.5**

The (mean) auto-correlation function for NKp landscapes ($N = 30$, $K = 4$) for various values of p .

**Figure 3.1.6**

The (mean) variance/covariance for NKp landscapes ($N = 30$, $K = 4$) plotted against p for various values of d , for sampled data and for the formula of Conjecture 3.1.2.

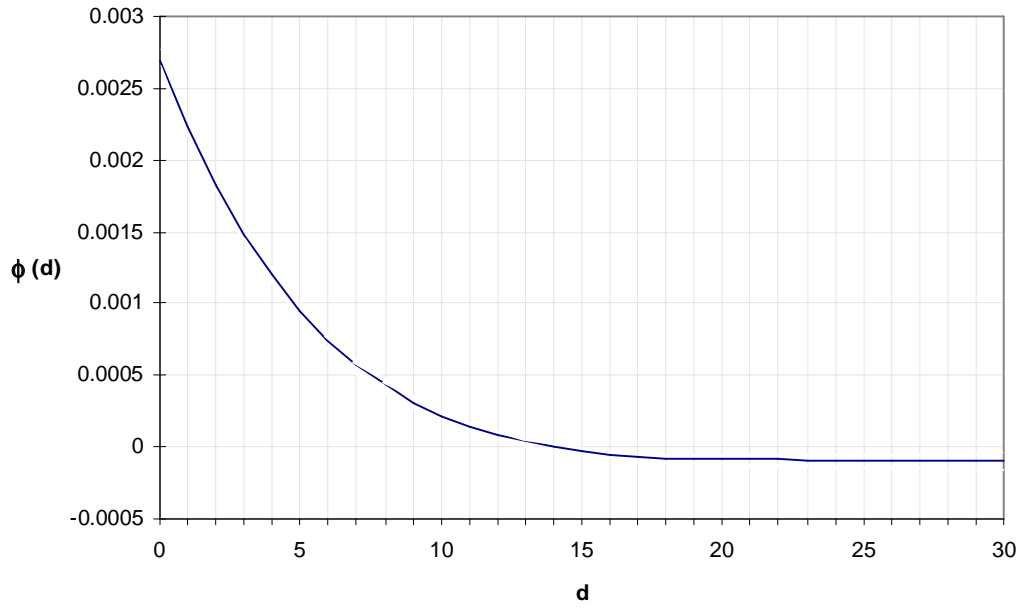


Figure 3.1.7

The factor $\phi_{N,K}(d)$ for the data from figure 3.1.6. Dotted lines represent \pm one standard deviation.

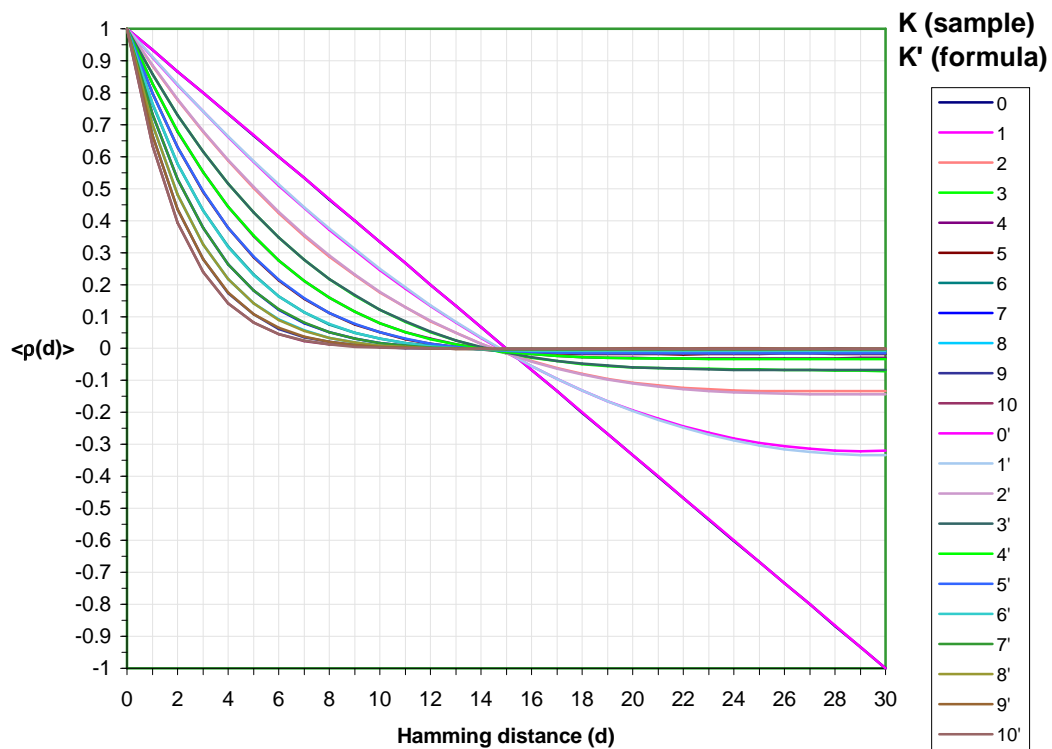


Figure 3.1.8

The (mean) auto-correlation for NKp landscapes ($N = 30$, $K = 0, \dots, 10$) with results from sampled data plotted alongside corresponding results calculated by the formula in Conjecture 3.1.3

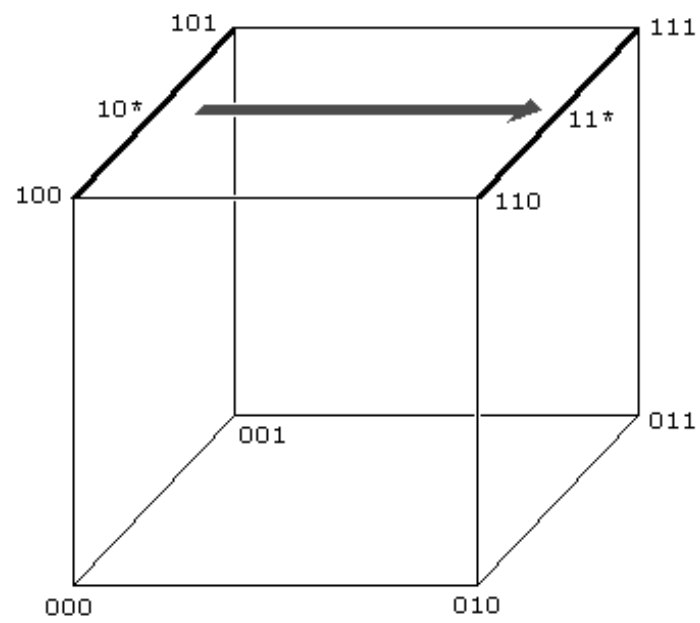
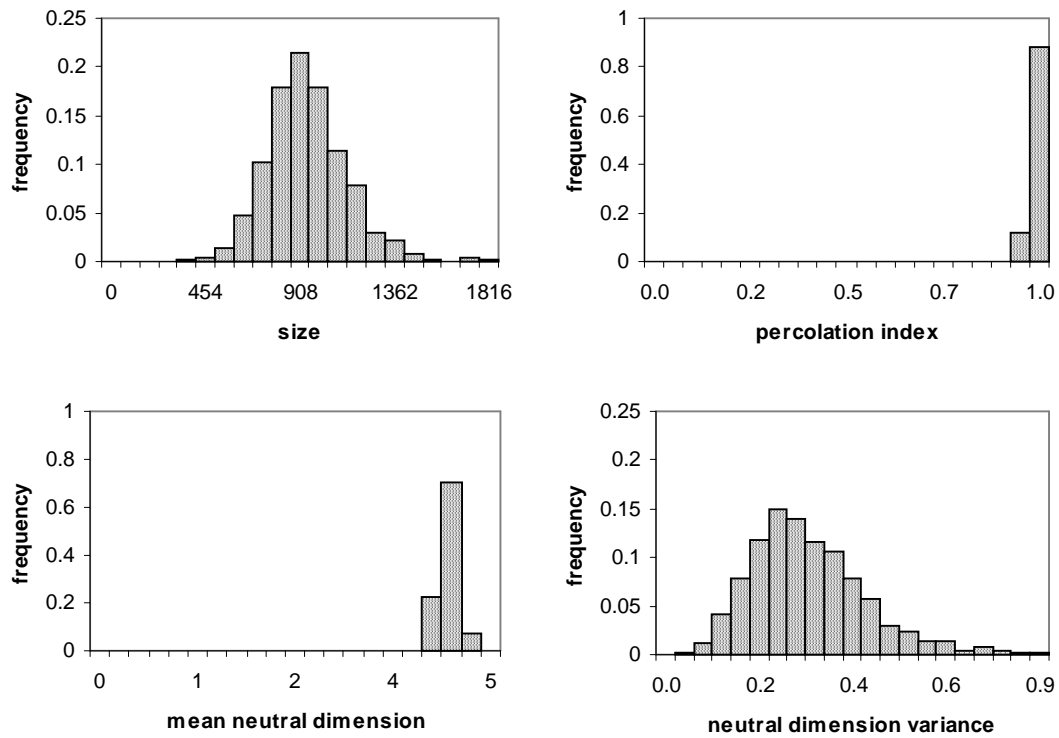
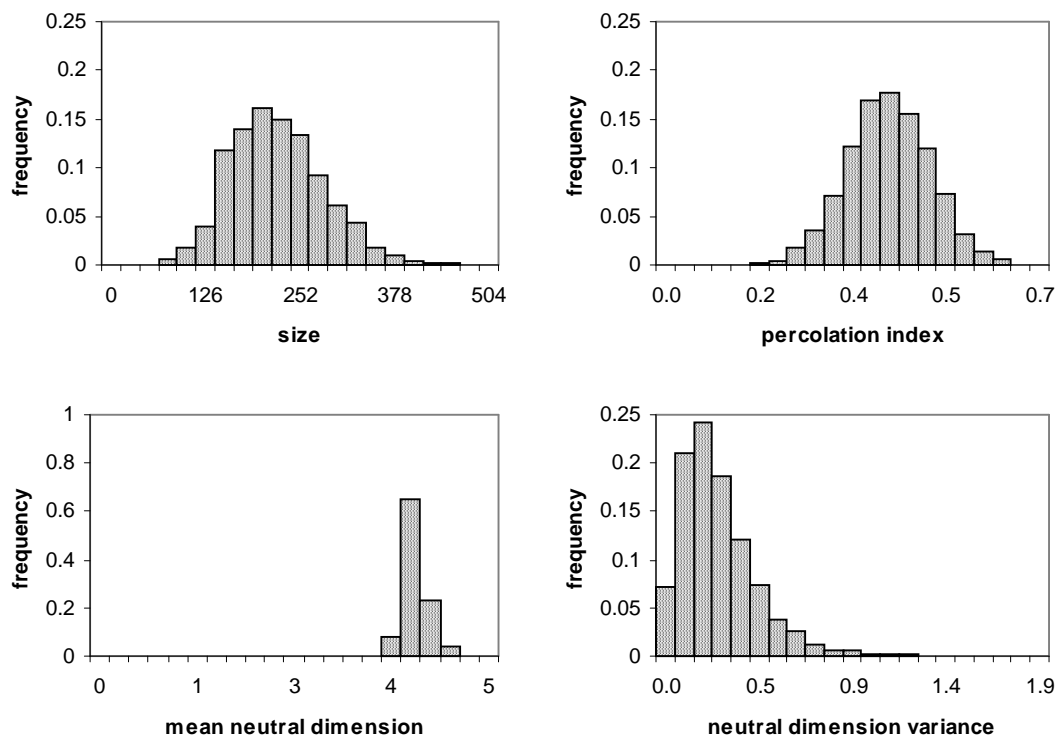


Figure 3.2.1

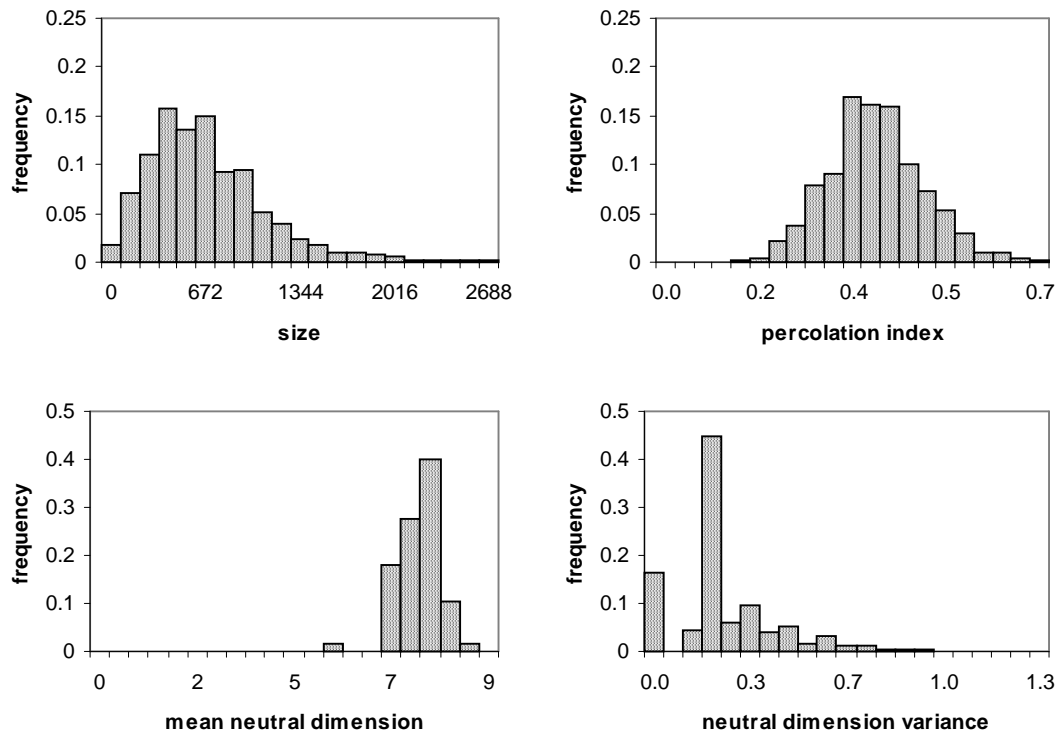
A 1-dimensional hypercube takes a step in Q^3

**Figure 3.2.2a**

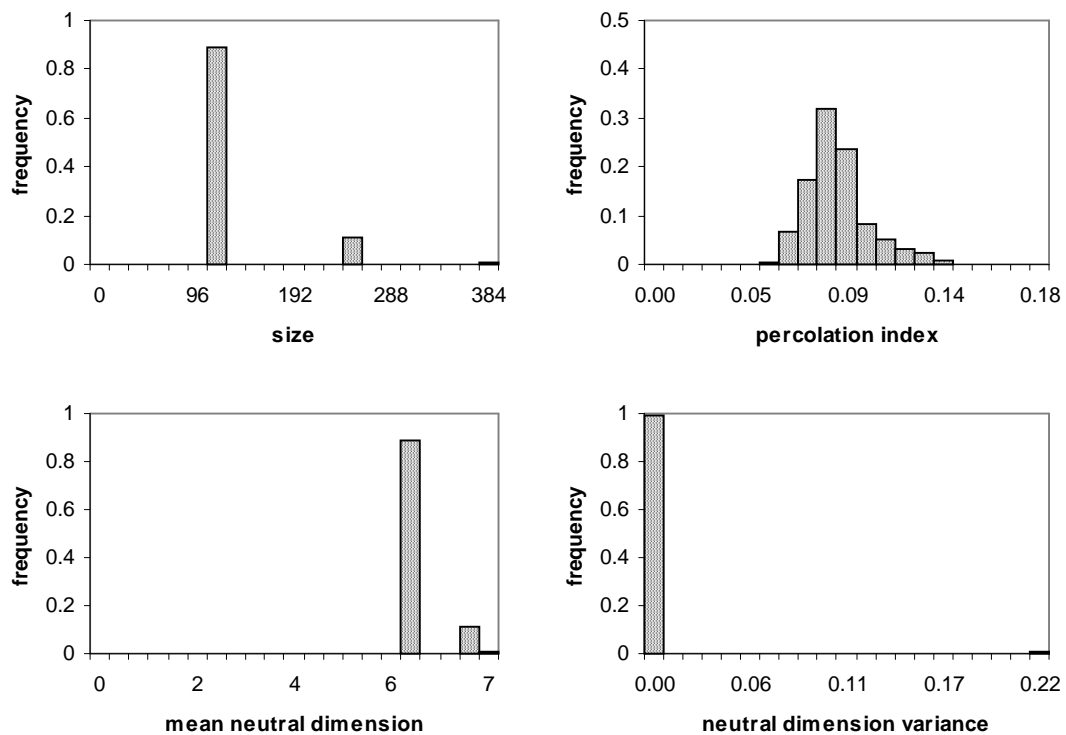
Neutral Network Statistics for RNN landscapes: $N = 18$, $R = 100$, $D = 4$

**Figure 3.2.2b**

Neutral Network Statistics for RNN landscapes: $N = 18$, $R = 500$, $D = 4$

**Figure 3.2.2c**

Neutral Network Statistics for RNN landscapes: $N = 18$, $R = 100$, $D = 8$

**Figure 3.2.2d**

Neutral Network Statistics for RNN landscapes: $N = 18$, $R = 500$, $D = 8$

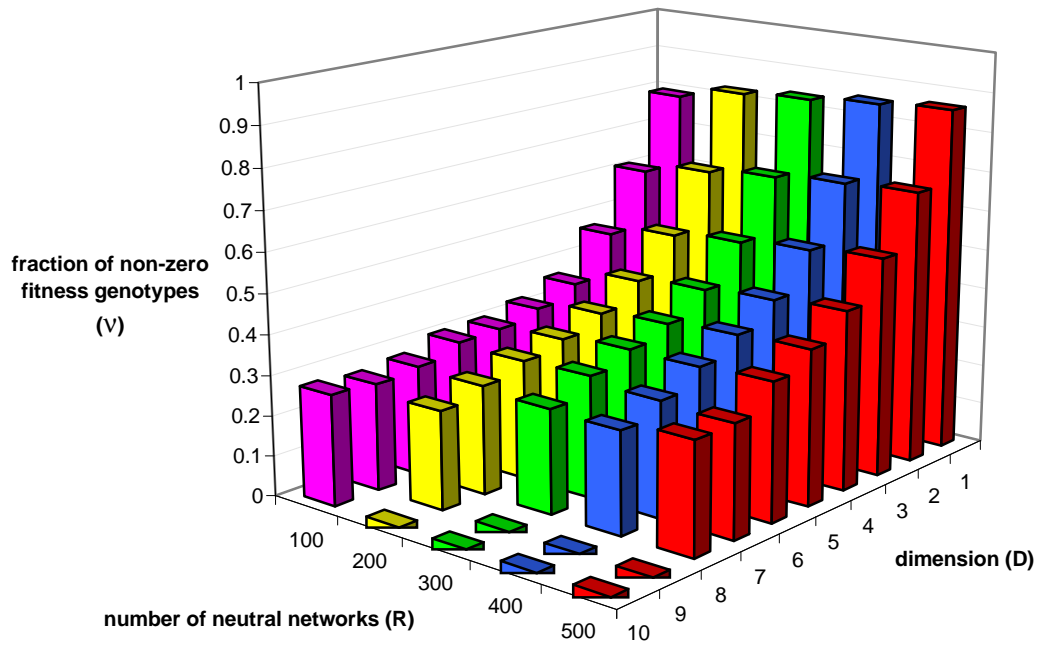


Figure 3.2.3

Fraction of RNN landscapes filled by (non-zero fitness) neutral networks for $N = 18$. Note: gaps indicate that the construction procedure failed (timed-out)

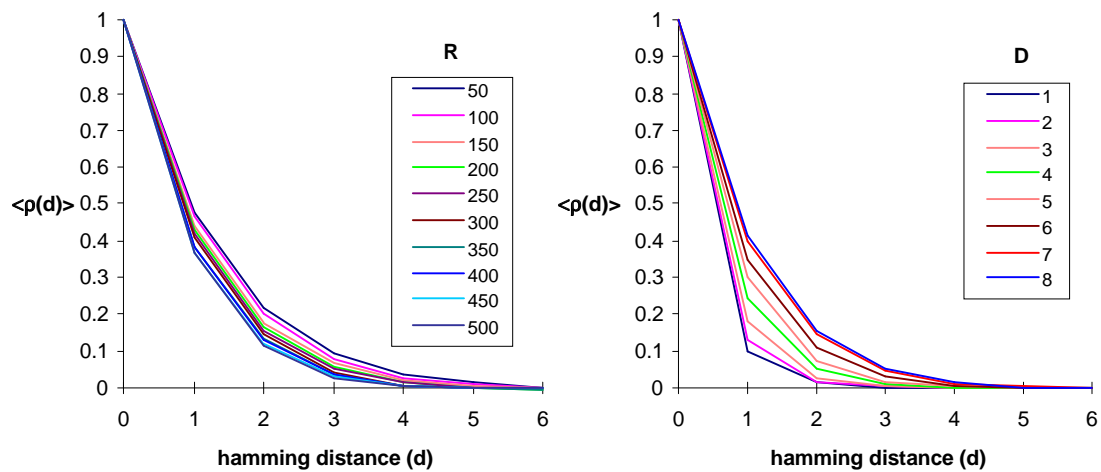


Figure 3.2.4a

Figure 3.2.4b

The (mean) auto-correlation function $\langle p(d) \rangle$ on RNN landscapes for $N = 18$. Figure 3.2.4a plots $\langle p(d) \rangle$ for $D = 8$ and $R = 50 - 500$. Figure 3.2.4b plots $\langle p(d) \rangle$ for $R = 250$ and $D = 1 - 8$.

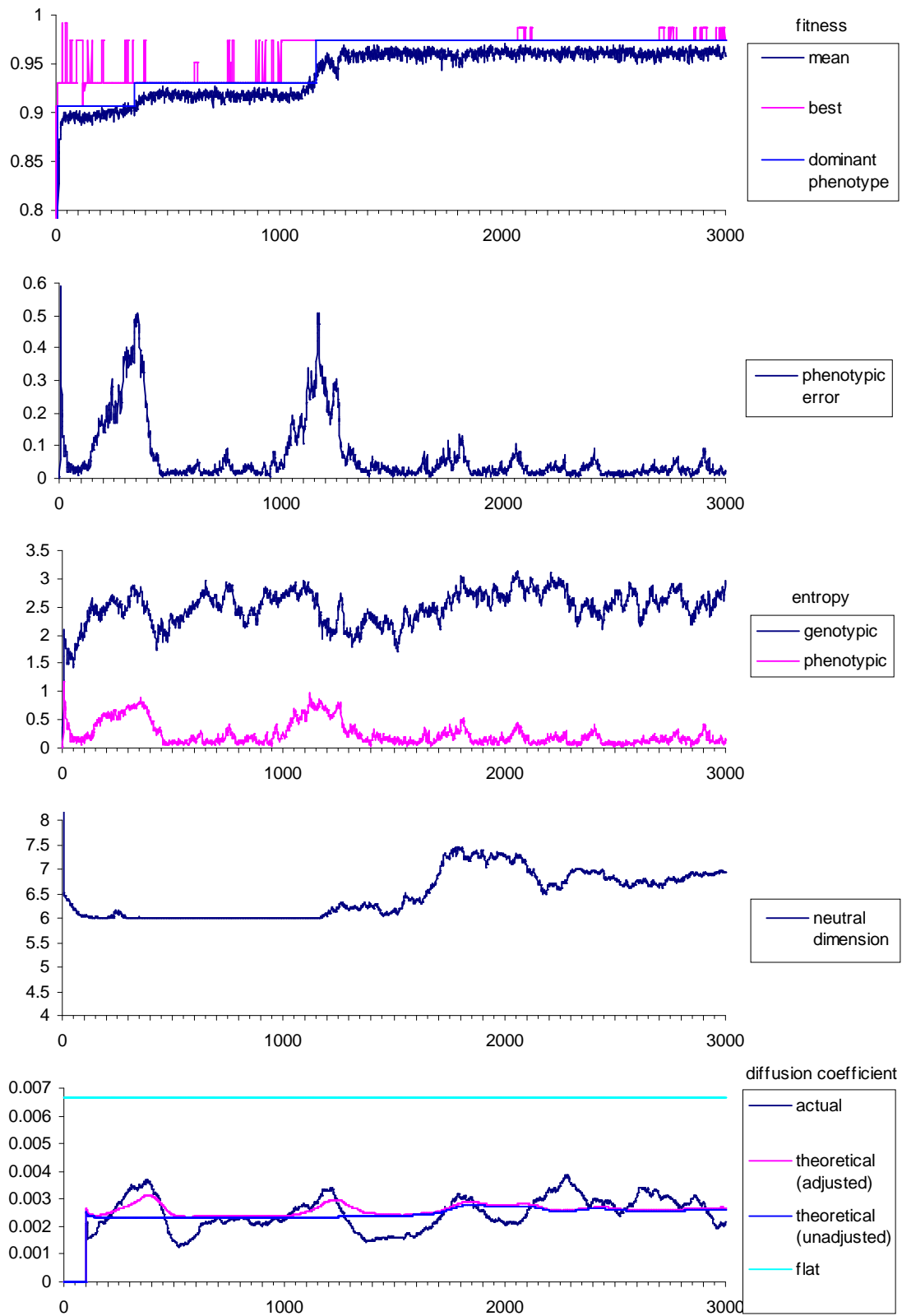
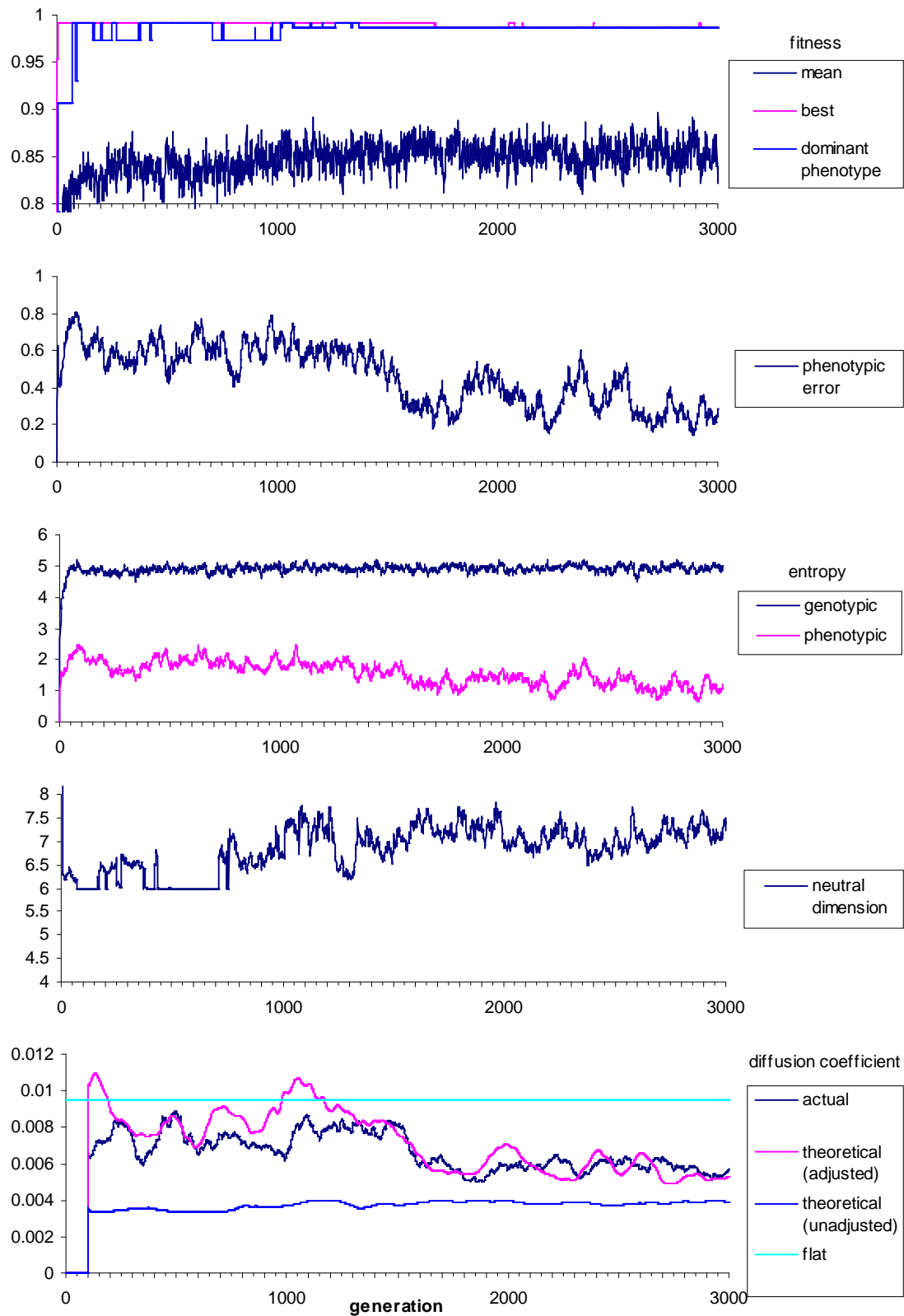
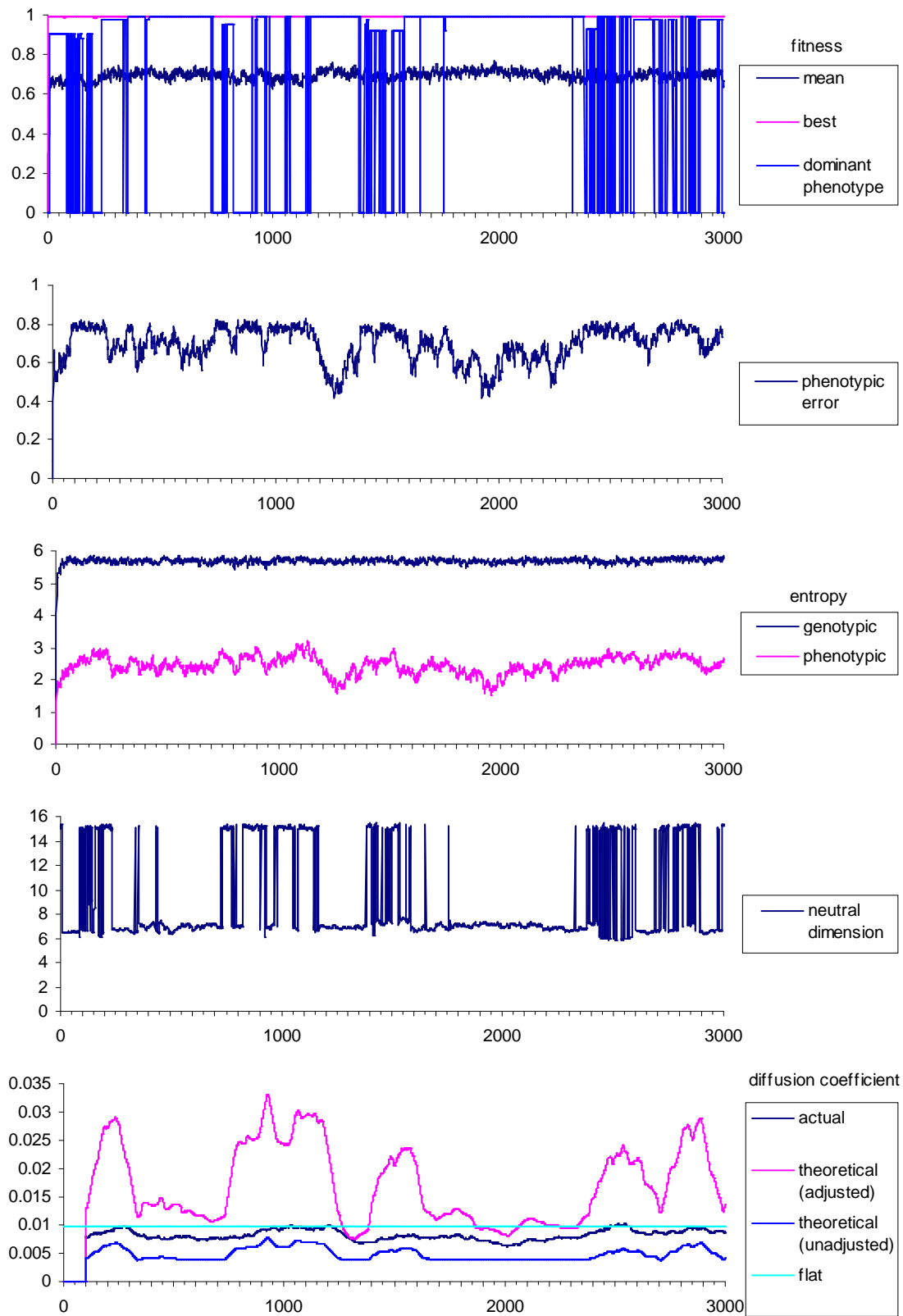


Figure 5.1.1

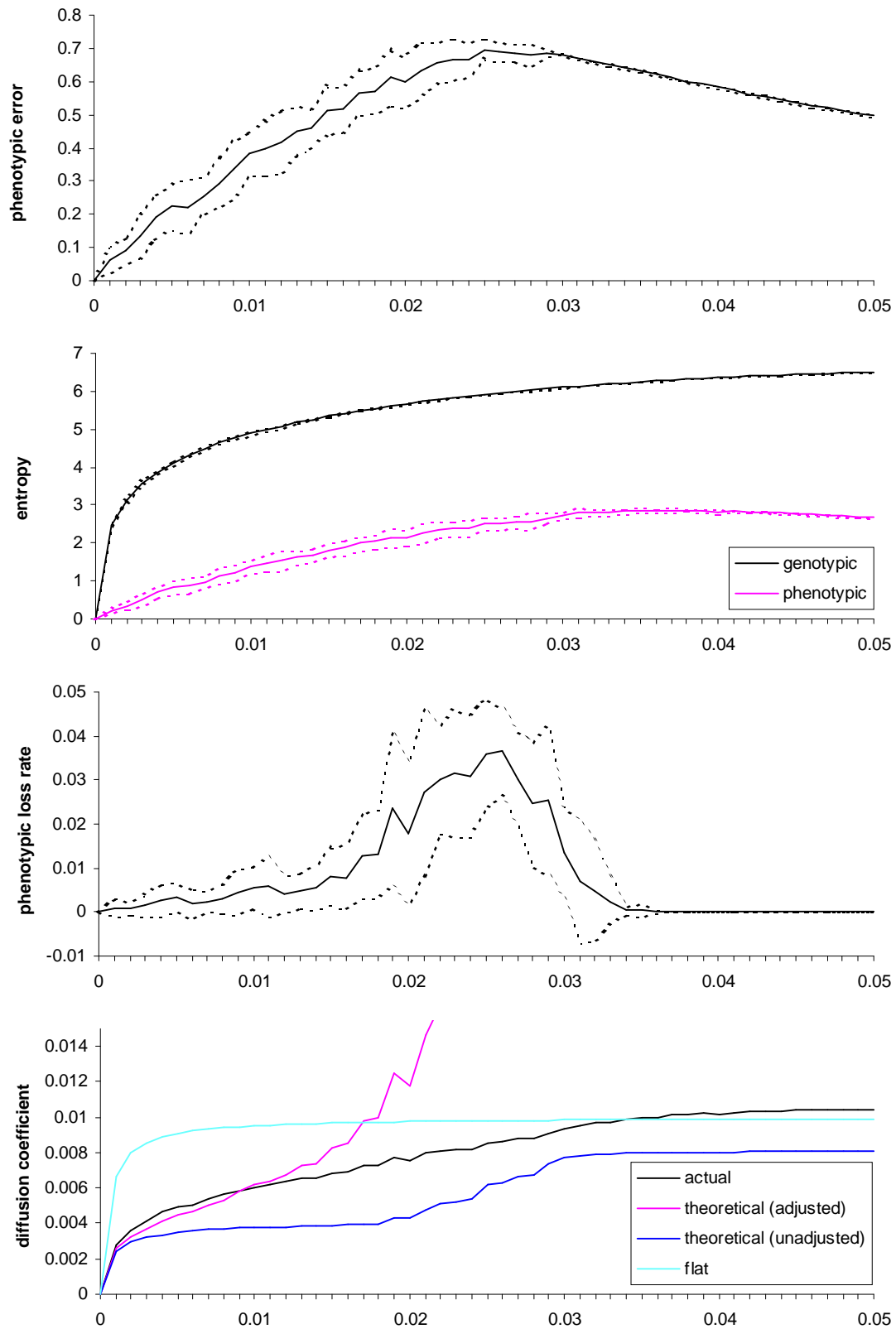
Population dynamics on an RNN Landscape: $N = 20$, $R = 100$, $D = 6$, population = 1000, mutation rate = 0.001 per locus. Abscissa is number of generations. Initial population is 1000 identical genotypes of fitness zero.

**Figure 5.1.2**

As Figure 5.1.1 except that the mutation rate is now 0.01.

**Figure 5.1.3**

As Figure 5.1.1 except that the mutation rate is 0.02.

**Figure 5.1.4**

Dependence of population dynamical measures on mutation rate (abscissa) for RNN landscapes with $N = 20$, $R = 100$, $D = 6$, population 1000. Figures are averages over the last 4500 generations of 20 runs of 5000 generations each. Dotted lines indicate ± 1 standard deviation.

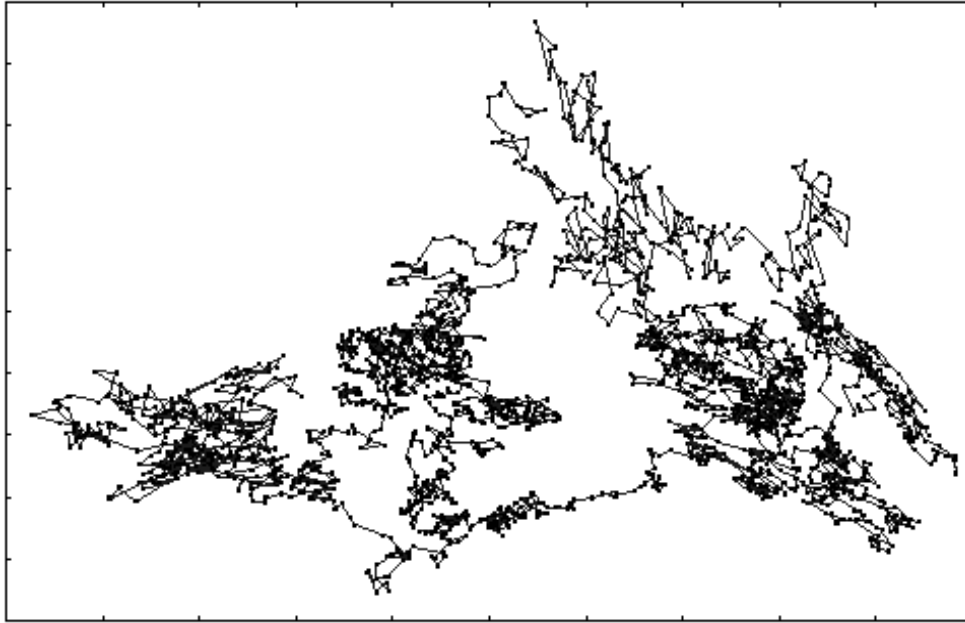


Figure 5.1.5

A Principal Components projection onto two dimensions of the path travelled by the centroid of a population evolving on an RNN landscape.

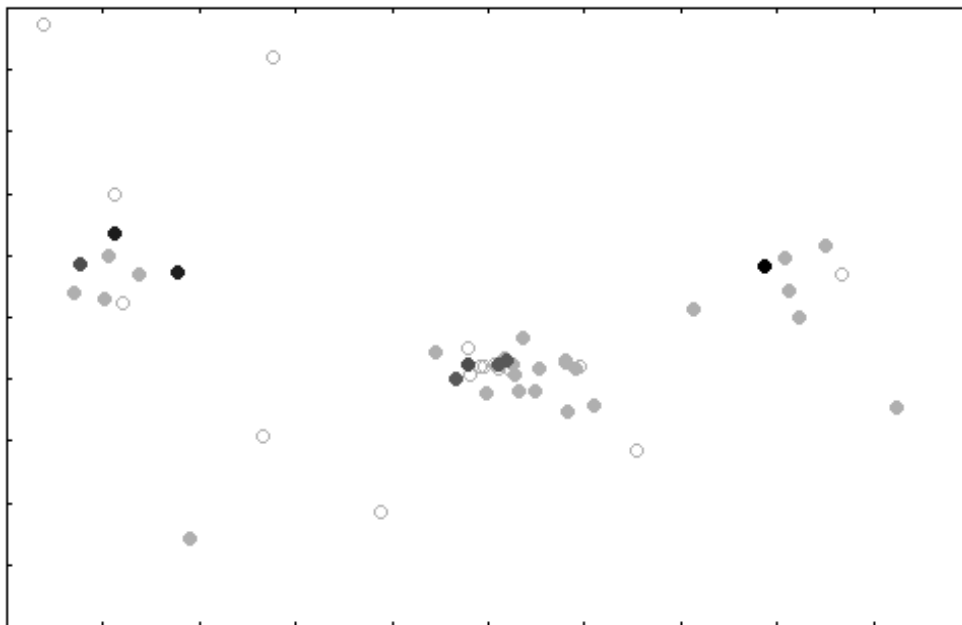


Figure 5.1.6

A Principal Components projection (using the algorithm specified in Section 4 IV) of a "snapshot" of the (genotypic) support of a population evolving on an RNN landscape (same run as Figure 5.1.5), illustrating clustering. Solid circles represent genotypes on the dominant neutral network, hollow circles genotypes not on the network. Colours represent the number of instances of genotypes; genotypes are banded by number in ascending order: grey, green, blue, red, black.

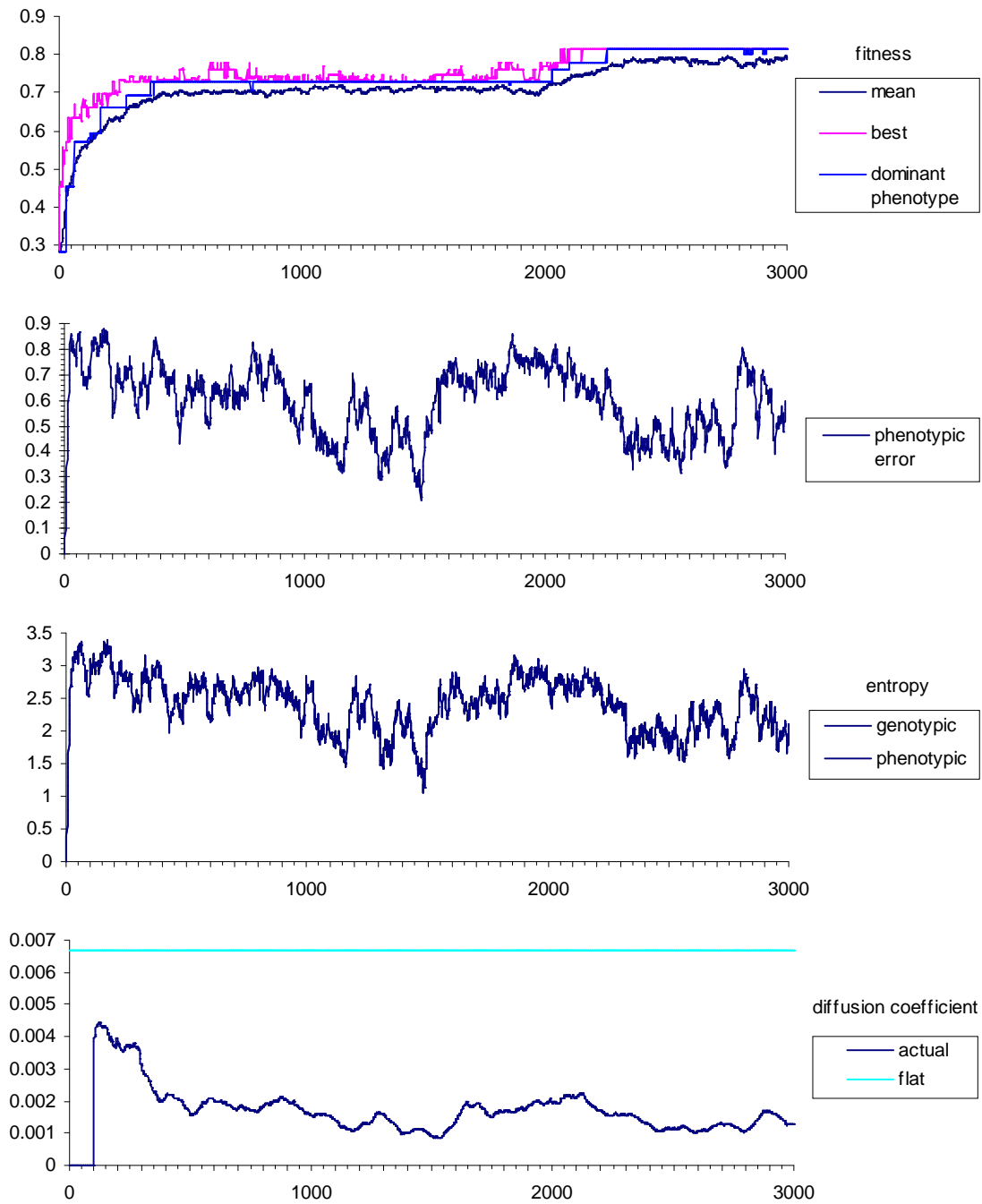
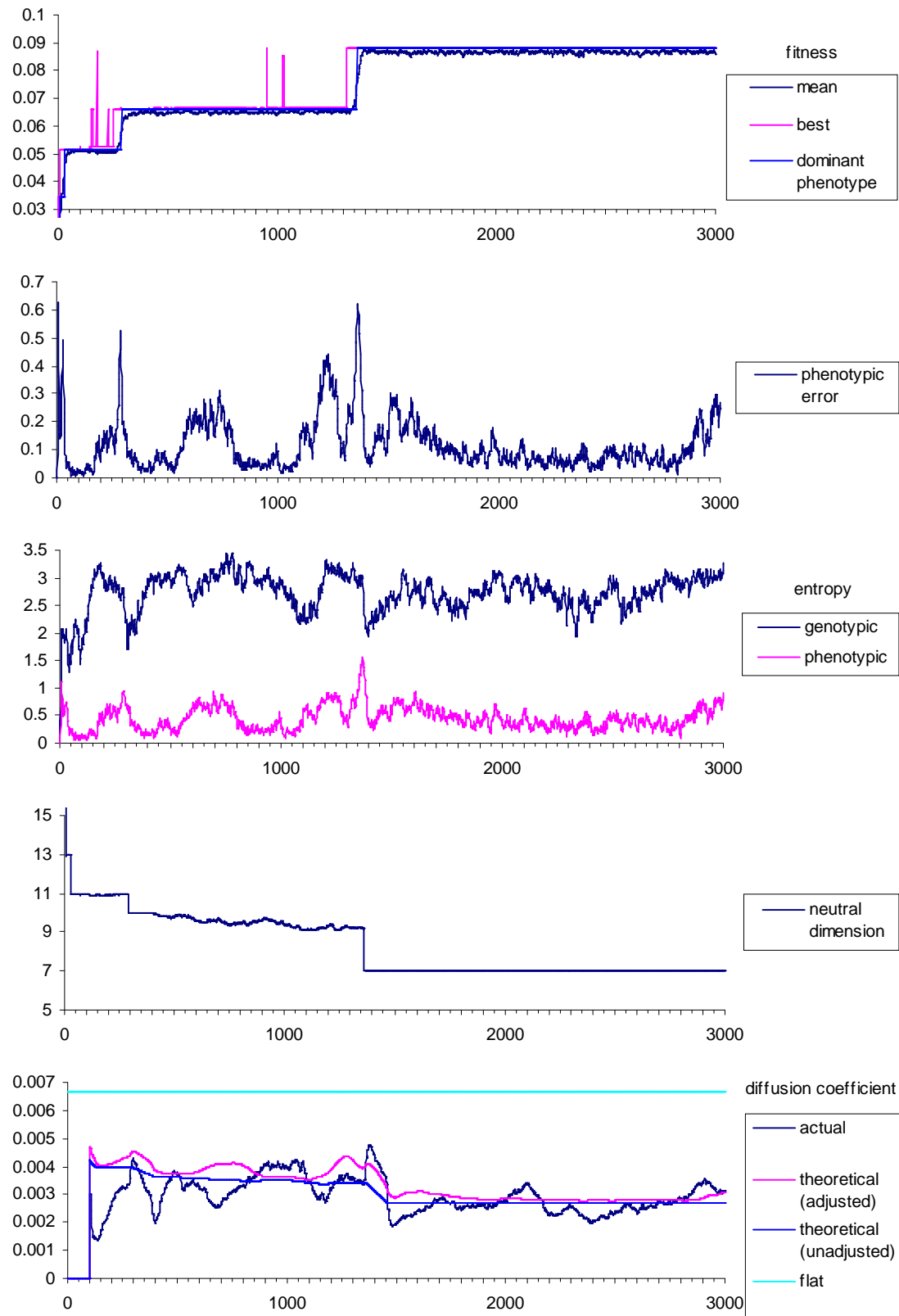


Figure 5.2.1

Population dynamics on an NKp Landscape: $N = 20$, $K = 4$, $p=0$, population = 1000, mutation rate = 0.001 per locus. Abscissa is number of generations. Initial population is 1000 identical genotypes of fitness \sim zero.

**Figure 5.2.2**

All parameters the same as in Figure 5.2.1, except that here $p = 0.99$

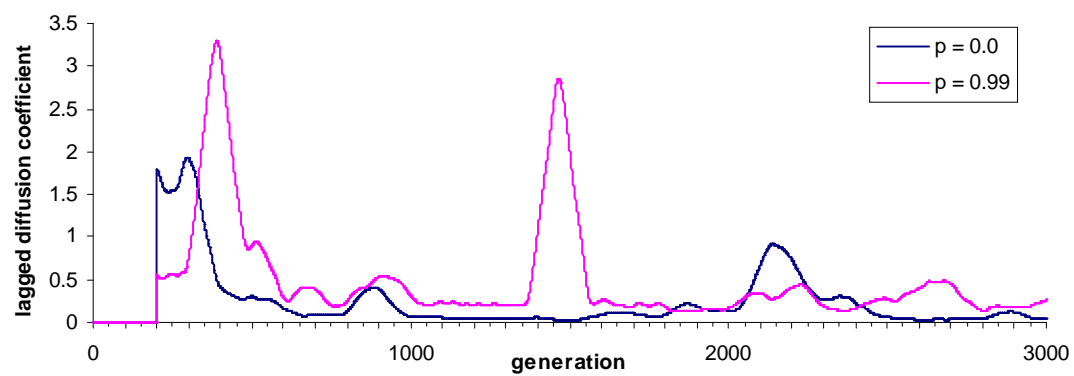


Figure 5.2.3

Comparison of lagged diffusion coefficients for the $p = 0$ and $p = 0.99$ runs.

APPENDIX A

A.1 Calculation of the probability that a mutation on an NKp landscape is neutral

Let us introduce the notation $i \rightarrow j$ to indicate that locus i is epistatically linked to locus j [this corresponds to a red arrow from locus i to locus j in Figure 3.1.1].

Let an NKp landscape be given and let g and g' be two genotypes differing by a single point mutation. Without loss of generality we take $g = 000 \dots 0$ (N zeros) and $g' = 100 \dots 0$ ($N-1$ zeros). We wish to calculate $p_{\text{neutral}} \equiv \mathbf{P}(f(g) = f(g'))$. It is clear that:

$$f(g) = f(g') \Leftrightarrow \text{for all loci } i \ \sigma_i(g) = \sigma_i(g') \text{ or } F_i(\sigma_i(g)) = F_i(\sigma_i(g')) = 0.$$

Note that this equivalence holds "almost surely", and that the "or" is not necessarily exclusive. Let us call the i -th condition on the r.h.s. of this statement A_i . It is clear (from the independent assignment of epistatic links and fitness table entries) that the conditions A_i are independent, so that

$p_{\text{neutral}} = \prod_{i=1}^N \mathbf{P}(A_i)$. Now for $i = 1$ we always have $\sigma_1(g) \neq \sigma_1(g')$, since $\sigma_1(g) = 000 \dots 0$ ($K+1$ zeros), while $\sigma_1(g') = 100 \dots 0$ (K zeros). Hence $\mathbf{P}(A_1) = \mathbf{P}(F_1(\sigma_1(g)) = F_1(\sigma_1(g')) = 0) = p^2$. For $i \neq 1$ we calculate $\mathbf{P}(A_i^C)$ (where A_i^C is the complement of A_i) as follows: we observe that $\sigma_i(g) \neq \sigma_i(g')$ iff $1 \rightarrow i$ (otherwise $\sigma_i(g)$ and $\sigma_i(g')$ both consist entirely of zeros). By the construction of an NKp landscape we have $\mathbf{P}(i \rightarrow j) = \frac{K}{N-1}$ for any i, j . Thus $\mathbf{P}(A_i^C) = 1 - \mathbf{P}(A_i) = \frac{K}{N-1}(1 - p^2)$. Putting everything together, we find:

$$\text{A.1.1} \quad p_{\text{neutral}} = p^2 \left(1 - \frac{K}{N-1}(1 - p^2) \right)^{N-1}$$

A.2 Calculation of the auto-correlation function for a "degenerate" NKp landscape

Consider the "degenerate" NKp landscape G where the epistatic links to locus 1 are itself and loci $2 \dots (K+1)$, and where the only non-zero entry in any of the fitness tables is $F_1(\sigma_0) = f_0$ where $\sigma_0 = 000 \dots 0$ ($K+1$ zeros).

Let us set $M \equiv |G| = 2^N$ and $P \equiv 2^{K+1}$. Define $G_0 \equiv \{g \in G \mid g_1 = g_2 = \dots = g_{K+1} = 0\}$. We have $|G_0| = 2^{N-K-1} = \frac{1}{P} M$ and $|G_0^C| = \left(1 - \frac{1}{P}\right) M$ where "C" denotes set complement.

We then have:

$$f(g) = \begin{cases} \frac{f_0}{N} & g \in G_0 \\ 0 & g \notin G_0 \end{cases}$$

The mean fitness is given by:

$$\begin{aligned}\bar{f} &= \frac{1}{M} \sum_{g \in G} f(g) \\ &= \frac{1}{M} \left(\sum_{g \in G_0} f(g) + \sum_{g \notin G_0} f(g) \right) \\ &= \frac{1}{P} \frac{f_0}{N}\end{aligned}$$

since the second sum vanishes. We re-write this as:

$$\mathbf{A.2.1} \quad f_0 = PN\bar{f}$$

The fitness variance is calculated as:

$$\begin{aligned}\sigma_f^2 &= \frac{1}{M} \sum_{g \in G} (f(g) - \bar{f})^2 \\ &= \frac{1}{M} \left(\sum_{g \in G_0} (f(g) - \bar{f})^2 + \sum_{g \notin G_0} (f(g) - \bar{f})^2 \right) \\ &= \frac{1}{P} (P\bar{f} - \bar{f})^2 + \left(1 - \frac{1}{P}\right) \bar{f}^2\end{aligned}$$

i.e.

$$\mathbf{A.2.2} \quad \sigma_f^2 = (P-1)\bar{f}^2$$

Let us set $G^2(d) \equiv \{(g, g') \in G \times G \mid h(g, g') = d\}$ for $d = 0, 1, 2, \dots, N$ where $h(\cdot, \cdot)$ is hamming distance. Then $|G^2(d)| = M \binom{N}{d}$ and the auto-correlation at distance d is given by:

$$\begin{aligned}\rho(d) &= \frac{1}{M \binom{N}{d} \sigma_f^2} \sum_{(g, g') \in G^2(d)} (f(g) - \bar{f})(f(g') - \bar{f}) \\ &= \frac{1}{M \binom{N}{d} \sigma_f^2} \left\{ \sum_{(g, g') \in G^2(d) \cap G_0 \times G_0} (f(g) - \bar{f})(f(g') - \bar{f}) + 2 \sum_{(g, g') \in G^2(d) \cap G_0 \times G_0^c} (f(g) - \bar{f})(f(g') - \bar{f}) + \sum_{(g, g') \in G^2(d) \cap G_0^c \times G_0^c} (f(g) - \bar{f})(f(g') - \bar{f}) \right\} \\ &= \frac{1}{M \binom{N}{d} \sigma_f^2} \left\{ \sum_{(g, g') \in G^2(d) \cap G_0 \times G_0} (P-1)^2 \bar{f}^2 - 2 \sum_{(g, g') \in G^2(d) \cap G_0 \times G_0^c} (P-1) \bar{f}^2 + \sum_{(g, g') \in G^2(d) \cap G_0^c \times G_0^c} \bar{f}^2 \right\}\end{aligned}$$

where we have used **A.2.1** to express $f(g)$, $f(g')$ in terms of \bar{f} .

Now let us set:

$$\begin{aligned} \alpha(d) &\equiv \frac{P}{M} \left| G^2(d) \cap G_0 \times G_0 \right| \\ \text{A.2.3} \quad \beta(d) &\equiv \frac{P}{M} \left| G^2(d) \cap G_0 \times G_0^c \right| \\ \gamma(d) &\equiv \frac{P}{M} \left| G^2(d) \cap G_0^c \times G_0^c \right| \end{aligned}$$

We then have:

$$\text{A.2.4} \quad \rho(d) = \frac{(P-1)^2 \alpha(d) - 2(P-1)\beta(d) + \gamma(d)}{P(P-1) \binom{N}{d}}$$

using A.2.2 and it remains to calculate $\alpha(d)$, $\beta(d)$ and $\gamma(d)$. Let us set $L \equiv N - K - 1$.

It is easy to see that:

$$\text{A.2.5} \quad \alpha(d) = \begin{cases} \binom{L}{d} & \text{if } d \leq L \\ 0 & \text{otherwise} \end{cases}$$

To calculate $\beta(d)$ consider the genotype $g = \overbrace{00\dots 0}^{K+1} b_1 b_2 \dots b_L$ - i.e. an arbitrary member of G_0 . For every element (g, g') of $G^2(d) \cap G_0 \times G_0^c$ g' is formed by flipping d bits of such a g in such a way that the result is in G_0^c - i.e. at least one of the $K+1$ zeros must be flipped. We count the number of ways this can be done. Now we can flip d bits of g in $\binom{N}{d}$ ways. But of these $\binom{L}{d}$ will have been formed by only flipping the b_i 's (if $d \leq L$), so that the result is still in G_0 . Thus we find that:

$$\beta(d) = \begin{cases} \binom{N}{d} - \binom{L}{d} & \text{if } d \leq L \\ \binom{N}{d} & \text{otherwise} \end{cases}$$

or

$$\text{A.2.6} \quad \beta(d) = \binom{N}{d} - \alpha(d)$$

To calculate $\gamma(d)$ consider the genotype $g = a_1 a_2 \dots a_{K+1} b_1 b_2 \dots b_L$ where at least one of the a_i 's is non-zero - i.e. an arbitrary member of G_0^c . For every element (g, g') of $G^2(d) \cap G_0^c \times G_0^c$ g' is formed by flipping d bits of such a g , in such a way that the result is in G_0^c - i.e. at least one of the a_i 's must still be non-zero. Again, we count the number of ways this can be done. Consider the case where exactly k of the a_i 's in g are non-zero to start with, for $k = 1, 2, \dots, K+1$ - there are $\binom{K+1}{k}$ such arrangements. For each of such a genotype there are $\binom{N}{d}$ ways of flipping d of its bits. But for some

of these, we will end up flipping precisely the k non-zero a_i 's. This will happen in $\binom{L}{d-k}$ cases (if $0 \leq d-k \leq L$). Thus we find:

$$\gamma(d) = \sum_{k=1}^{K+1} \binom{K+1}{k} \left[\binom{N}{d} - \begin{cases} \binom{L}{d-k} & d-L \leq k \leq d \\ 0 & \text{otherwise} \end{cases} \right]$$

or

$$\mathbf{A.2.7} \quad \gamma(d) = (P-1) \binom{N}{d} - \sum_{\text{Max}(1, d-L) \leq k \leq \text{Min}(d, K+1)} \binom{K+1}{k} \binom{L}{d-k}$$

The result is now given by **A.2.4**, using **A.2.5**, **A.2.6** and **A.2.7**.